SYNTHESIS OF SELENIUM-INCORPORATED ALPHA-TRICALCIUM PHOSPHATE AND EVALUATION OF ITS CEMENT-TYPE REACTIVITY

A THESIS SUBMITTED TO
THE GRADUATE SCHOOL OF NATURAL AND APPLIED SCIENCES
OF
MIDDLE EAST TECHNICAL UNIVERSITY

BY

BERSU BAŞTUĞ AZER

IN PARTIAL FULFILLMENT OF THE REQUIREMENTS
FOR
THE DEGREE OF MASTER OF SCIENCE
IN
METALLURGICAL AND MATERIALS ENGINEERING

JANUARY 2019

Approval of the thesis:

SYNTHESIS OF SELENIUM-INCORPORATED ALPHA-TRICALCIUM PHOSPHATE AND EVALUATION OF ITS CEMENT-TYPE REACTIVITY

submitted by **BERSU BAŞTUĞ AZER** in partial fulfillment of the requirements for the degree of **Master of Science in Metallurgical and Materials Engineering Department, Middle East Technical University** by,

Prof. Dr. Halil Kalıpçılar
Dean, Graduate School of **Natural and Applied Sciences** _____

Prof. Dr. Cemil Hakan Gür
Head of Department, **Met. and Mat. Eng.** _____

Prof. Dr. Caner Durucan
Supervisor, **Met. and Mat. Eng., METU** _____

Examining Committee Members:

Prof. Dr. Arcan Fehmi Dericioğlu
Metallurgical and Materials Engineering Dept., METU _____

Prof. Dr. Caner Durucan
Met. and Mat. Eng., METU _____

Prof. Dr. Burcu Akata Kurç
Micro and Nanotechnology Dept., METU _____

Assist. Prof. Dr. Simge Çınar
Metallurgical and Materials Engineering Dept., METU _____

Assoc. Prof. Dr. Ziya Esen
Material Science and Engineering Dept., Çankaya University _____

Date: 31.01.2019

I hereby declare that all information in this document has been obtained and presented in accordance with academic rules and ethical conduct. I also declare that, as required by these rules and conduct, I have fully cited and referenced all material and results that are not original to this work.

Name, Surname: Bersu Baştuğ Azer

Signature:

ABSTRACT

SYNTHESIS OF SELENIUM-INCORPORATED ALPHA-TRICALCIUM PHOSPHATE AND EVALUATION OF ITS CEMENT-TYPE REACTIVITY

Başţuğ Azer, Bersu
Master of Science, Metallurgical and Materials Engineering
Supervisor: Prof. Dr. Caner Durucan

January 2019, 69 pages

In the case of bone defects and damages synthetic bone grafts have been widely used for filling the demaged parts. Alpha-tricalcium phosphate (α-TCP) is an attractive calcium orthophosphate as replacement of hard tissues. It converts from powder form to hardened apatite, by cement-type reaction in aqueous solutions, which is therefore a promising hard bone tissue analog and clinically used in bone defect filling operations. In this concept adding therapeutic function to the hardened cement products is an additional challenge and research interest. When compared with organic durgs and proteins, metallic ions are promising therapeutic agents because of their high availability and stability. In order to improve the therapeutic properties of α-TCP, various metallic ions can be incorporated. In this study, selenium (Se) ion has been incorporated to α-TCP to give anti-carcinogenic effect. Se-incorporated α-TCP (α-TCP:Se) has been synthesized by the solid-state reaction of custom synthesized Se-incorporated monetite ($CaHPO_4$:Se) and calcium carbonate ($CaCO_3$). The microstructural and morphological properties of as synthesized α-TCP products with different amounts of Se-incorporation remain unaffected by doping. Up to 2 wt. % Se-incorporation, the only phase obtained from the XRD analyses is α-TCP, however, higher than 2 wt. % Se-incorporation to α-TCP leads to formation of the

hydroxyapatite (HAp) together with α-TCP. Complete cement-type conversion from α-TCP to calcium-deficient hydroxyapatite (CDHAp) has been performed with pure and different amount of Se-incorporated α-TCP products. The hydration kinetics of cement-type conversion is positively changed with the presence of Se. Higher amount of Se addition slows down the kinetics of cement-type conversion. The morphological properties are remained same for Se-incorporated and pure α-TCP. Less than 2 wt. % Se doping is critical limit for obtaining only α-TCP without formation of any other calcium phosphates and it's critical for faster hydration kinetics of cement conversion reaction from α-TCP to CDHAp.

Keywords: Bioceramics, Alpha-Tricalcium Phosphate, Bone Cements, Therapeutic Agent, Metallic Ion, Selenium

ÖZ

SELENYUM KATKILI ALFA-TRİKALSİYUM FOSFAT SENTEZİ VE ÇİMENTO TİPİ REAKTİVİTESİNİN DEĞERLENDİRİLMESİ

Baştuğ Azer, Bersu
Yüksek Lisans, Metalurji ve Malzeme Mühendisliği
Tez Danışmanı: Prof. Dr. Caner Durucan

Ocak 2019, 69 sayfa

Sentetik kemik grefleri kemik hasarları durumunda tahrip olmuş parçaları doldurmak için yaygın olarak kullanılmaktadır. Alfa-trikalsiyum fosfat (α-TCP), sert dokuların yerine konulmasında yaygın olarak kullanılan çekici bir kalsiyum ortofosfattır. Çimento tipi reaksiyonla sulu çözeltilerde ve vücut sıcaklığında, sert kemik dokusu iyileştirici madde olan ve kemik defekti doldurma işlemlerinde kullanılan apatit çimentosuna dönüşür. Son zamanlarda sertleşmiş çimento ürünlerinin terapötik etkisinin geliştirilmesi, bu konsept içinde incelenmektedir. Metalik iyonlar, organik ilaçlarla ve proteinlerle karşılaştırıldığında, yüksek kullanılabilirlik ve kararlılıklarından ötürü umut vaat eden terapötik ajanlardır. α-TCP'ın terapötik özelliklerini geliştirmek için çeşitli metalik iyonlar katkılanmaktadır. Bu tez çalışmasında, bu amaç için Selenyum (Se) iyonu, anti-kanserojen etki sağlamak için α-TCP'a katılmaktadır. Se-katkılı α-TCP (α-TCP:Se), özel olarak sentezlenmiş monetit ($CaHPO_4$:Se) ve kalsiyum karbonatın ($CaCO_3$) katı hal reaksiyonu ile sentezlenmiştir. Farklı miktarlarda Se eklenerek sentezlenmiş α-TCP ürünlerinin mikroyapısal ve morfolojik özelliklerinin katkılamadan etkilenmemektedir. %2'ye kadar Se-katkılanmasıyla XRD analizlerinden elde edilen tek faz α-TCP'dır, fakat ağırlıkça %2'den fazla Se-katkılanması α-TCP ile hidroksiapatit (HAp) oluşumuna yol açmaktadır. α-TCP'den kalsiyumca eksik hidroksiapatit (CDHAp) çimento tipi

dönüşüm reaksiyonu katkısız ve farklı miktarlarda Se içeren α-TCP ürünleri ile yapılmıştır. Çimento tipi dönüşümün hidrasyon kinetiği Se'nin varlığı ile olumlu olarak değişmiştir. Ağırlıkça daha fazla Se eklenmesi çimento tipi dönüşüm kinetiğini yavaşlatmaktadır. Se-katkılı ve saf α-TCP için morfolojik özellikler aynı kalmaktadır. Ağırlıkça %2'den daha az Se-katkısı, başka herhangi bir kalsiyum fosfat ürünü oluşmaksızın sadece α-TCP elde etmek için ve α-TCP'den CDHAp'a çimento-tipi reaksiyonu daha yüksek hidrasyon kinetiğine sahip olduğu için kritik sınır olarak belirlenmiştir.

Anahtar Kelimeler: Biyoseramikler, Alfa-Trikalsiyum Fosfat, Kemik Çimentoları, Terapötik Ajan, Metalik İyon, Selenyum

To my husband and my parents

ACKNOWLEDGMENTS

I would like to express my sincere appreciation to my supervisor Prof. Dr. Caner Durucan for his supervision, patience, motivation, guidance, advice, criticism, support and insight not only throughout this thesis but in many other studies.

I am greatful to my labmate Ekim Saraç and colleagues Elif Yeşilay, Başar Süer, Olgun Yılmaz, Cansu Savaş Uygur, Kadir Özgün Köse, Merve Özdil, Özgür Darıcıoğlu, Berk Aytuna for their support and friendship.

I am surely greatful to Assist. Prof. Dr. Simge Çınar for teaching and helping FTIR analysis techniques and her support in this study.

I want to express my gratitude to all the staff of the Department of Metallurgical and Materials Engineering especially; Yusuf Yıldırım for helping all quenching operation, Serkan Yılmaz for teaching electron microscopy techniques Gökhan Polat for teaching XRD analysis and Nilüfer Özel for her help in XRD analysis.

I am very greatful to my childhood friends Aylin Dedeoğlu and Ece Naz Yurtseven and my college friend Sıla Coşkun for their unconditional friendship and sharing everything in my life.

Finally, I owe a depth to my mom and dad for their unlimited support, unconditional love and their always similing faces and I feel deeply greatful to my husband, love of my life Mesutcan Azer for his care, support, endless love, showing me the ligth even in the darkest times not only throughout my master's education but in whole my life.

I sincerely want to dedicate this thesis to my husband and my parents for their support through the sleepless days and nights and their unconditional love.

TABLE OF CONTENTS

LIST OF TABLES

TABLES

LIST OF FIGURES

FIGURES

LIST OF ABBREVIATIONS

α-TCP	alpha-tricalcium phosphate
HAp	hydroxyapatite
CDHAp	calcium-deficient hydroxyapatite
$CaHPO_4$:Se:5wt.%	5 wt.% Se-incorporated $CaHPO_4$
$CaHPO_4$:Se:10wt.%	10 wt.% Se-incorporated $CaHPO_4$
α-TCP:Se:low	lower amount of Se-incorporated α-TCP
α-TCP:Se:high	higher amount of Se-incorporated α-TCP
CDHAp:Se:low	lower amount of Se-incorporated CDHAp
CDHAp:Se:high	higher amount of Se-incorporated CDHAp
β-TCP	beta-tricalcium phosphate
CaP	calcium phosphate
CPC	calcium phosphate cement
TTCP	tetracalcium phosphate
OCP	octacalcium phosphate
ACP	amorphous calcium phosphate
MCPM	monocalcium phosphate monohydrate

CHAPTER 1

INTRODUCTION

Nowadays, metals, ceramics and polymers have been used in different biomedical applications, such as bone implant, bone fracture repair and bone injury filling device. The most important issue in the design of these materials is to provide biocompatibility of the natural bone with compatible structural and mechanical properties with natural bone.

In this regard, natural or synthetic bone cements have been used as fillers for years to treat minor damages caused by trauma, natural aging and complications (fracture, tumor, etc.). The filling materials taken from the patient or the donor are obtained incommodiously and in a limited time. Moreover, there are some risks such as transport of the disease from the donor. Because of these difficulties, synthetic alternatives of biocompatible bone cements have used to augment these defects. Synthetic bone cements are inserted by the operation to the damaged side in paste form. It has a self-setting nature and converts into a hardened mass in the defected side. Acrylic-based polymeric polymethlymethacyrlate (PMMA) cements were the first generation bone cements. PMMA cements are formed by polymerization reaction of MMA monomer. However, the release of unreacted MMMA polymers and their highly exothermic nature of polymerization reaction pose some risks such as bone necrosis. Because of the given limitations of PMMA cements, bioactive and bioresorbable materials that adhere to the natural bone and provide new bone formation are more promising candidates for bone cement applications. As a result, calcium phosphate cements (CPC) have been developed and clinically used.

Ceramic-based CPCs are synthetic analogs that have higher functionality with respect to their biocompatibility and chemical similarity to mineral phase of natural

bone which is carbonated, calcium-deficient form of hydroxyapatite (HAp, $Ca_{10}(PO_4)_6(OH)_2$. In addition, the hardening mechanism of CPCs is more suitable in terms of physiological compatibility than acrylic-based polymers which are hardened by polymerization reaction.

Calcium phosphate cements are formed by mixing one or more calcium phosphate powders with an aqueous solution and they firstly form a paste in a few minutes then the paste is able to set and harden after being implanted within body. There are two calcium phosphate cement-end products; apatite and brushite cements. Brushite cements are produced by combining an acidic calcium phosphate powder with a relatively basic calcium phosphate powder in an aqueous solution to obtain neutral calcium phosphate cement. Apatite cements are more promising cement systems because the hardened end product of cement reaction resembles to the inorganic mineral phase of natural bone, biological apatite, in terms of chemical and structural properties. The most commonly preferred calcium phosphate compound to obtain apatite cement end product is α-tricalcium phosphate (α-TCP, α-$Ca_3(PO_4)_2$). When α-TCP is mixed with aqueous solution, it transforms into hardened calcium-deficient hydroxyapatite (CDHAp, $Ca_9(HPO_4)(PO_4)_5(OH)$). Unlike PMMA, CPCs do not harden by polymerization reaction and small amount of heat is released during hardening. These conversion reactions take place at physiological temperature, i.e. body temperature, 37 °C. The most important part is that the hardened cement-end product, calcium-deficient form of hydroxyapatite resembles the natural bone more than the stochiometric form. Moreover, CDHAp has higher solubility than stochiometric HAp, therefore, degradation rate of CDHAp is higher than HAp. In the clinical applications, CDHAp degrades and provides new bone tissue generation.

However, because of their ceramic origin, CPCs have poor mechanical properties. They are brittle and have low fracture toughness. Therefore, they are used in non-load bearing and maxillofacial hard tissue implant applications. In order to improve their mechanical properties, they are reinforced by inorganic compounds or biodegradable polymers to form composite cements.

In addition to their mechanical properties, cement-type reaction from α-TCP to CDHAp cement shows slower reaction kinetics than clinical requirements. By modifying the particle size, crystallinity, addition of certain chemicals, the reaction time and reaction kinetics can be changed.

Despite their disadvantages, because of their injectability and biodegradability, CPCs are not only used as bone substitutes, but also as drug-carrying materials. In contrast to other materials, the drugs are not only absorbed on the surface of the CPCs, but also attack the whole volume of the material. Nowadays, the most commonly, CPCs are combined with antibiotics, but anti-inflammatory drugs, anti-cancer drugs, and hormones are also incorporated into CPCs. However, because of some limitations of drugs, metallic ion incorporation into CPCs is more attractive for therapeutic purposes. When used in proper doses, metallic ion-substituted CPCs are able to show therapeutic effects without leading any toxicity to surrounding tissue. The metallic ion of selenium is a promising substitute ion because it exhibits in human immune systems as selenoproteins with their antioxidant function. Therefore, selenium have been used in anti-cancer orthopedic applications as selenite substituted HAp powders, selenium coated titanium implant. Selenium substituted calcium phosphate cement systems have not been synthesized yet in the literature.

In this thesis, pure and selenium-incorporated α-TCPs were synthesized by solid-state reaction. The effect of selenium addition to chemical properties, phases in the structure and morphological investigation were performed to pure and different amounts of Se-incorporated α-TCP powders. After complete characterization, these powders were converted to CDHAp cement by cement-type reaction at physiological temperature. The effect of selenium addition to hydration kinetics was investigated by isothermal calorimetry. The complete characterization in terms of microstructural investigation, phase identification, chemical properties were done for pure and Se-incorporated hardened cement-end products.

CHAPTER 2

LITERATURE REVIEW

2.1. Composition, structure and properties of natural bone

Bone, which is a mineralized tissue, has a primary function of "load carrying". Bone is a composite material, which is composed of three major components; 20 wt. % of organic matrix (90-96 % of organic matrix is collagen), 69 wt. % of mineral (which is calcium phosphate based mineral) and 9 wt. % of water. About 98 wt. % of bone is composed of non-living inorganic and organic parts which are listed. While 2 wt. % of bone is the living constituents which are osteoblasts (bone forming cells), osteoclasts (bone resorbing cells) and osteocytes [1].

According to Weiner et al. [2], the human lamellar bone has two distinct components; ordered and disordered materials. Ordered material forms the elementary unit of bone which is the mineralized collagen fibril. The collagen comprises the three dimensional matrix of the bone and reinforced by the inorganic, i.e. mineral part with aligned arrays. On the other hand, disordered material is formed by mineral matrix with poorly oriented collagen fibrils. Moreover, disordered material is also composed of non-collagenous organic material with small amount of water [3]. Figure 2.1 shows the 7 levels of hierarchical structure of bone starting from level 1, which is in nano scale, to level 7, which is in macro scale.

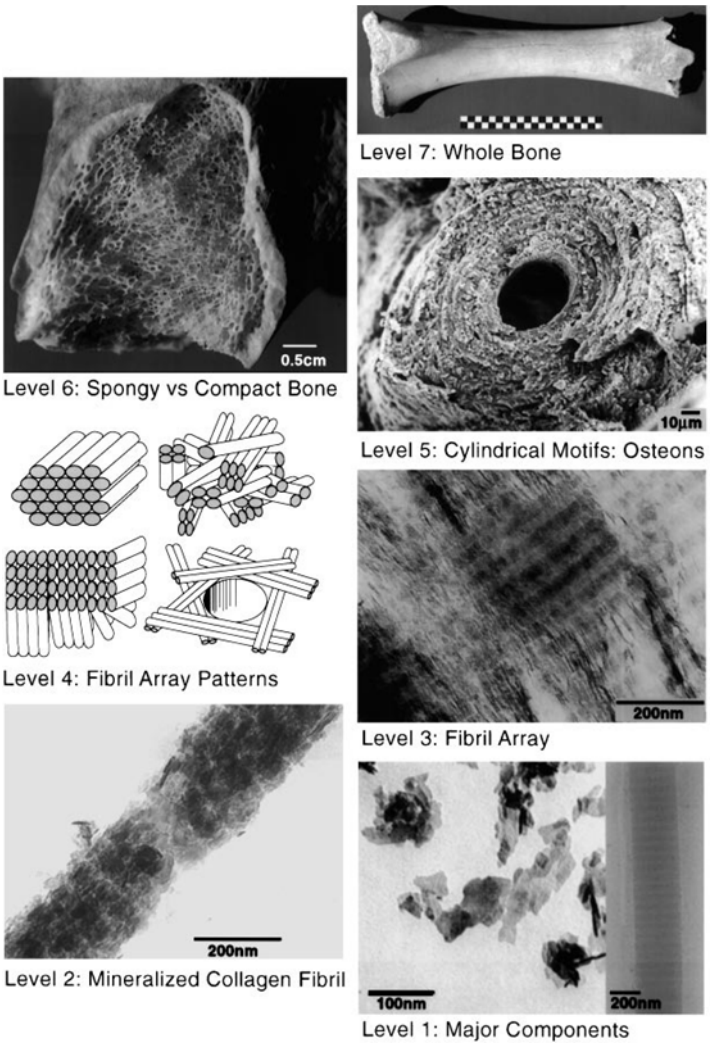

Figure 2.1 Schematic illustration of 7 levels of hierarchic constituents of bone [2].

Main organic component of natural bone is Type I collagen, but it is not the only protein, there are hundreds of non-collagenous proteins with less than 10 wt. % of the total organic part of the bone. Type I collagen presents as fibrils in bone with about 80-100 nm in diameter. About 1000 amino acids long three polypeptide chains form each fibril. These fibrils wound together in a triple helix with cylindrical shape with an approximate diameter of 1.5 nm and length of 300 nm. The unique fibril structure has a 67 nm periodicity. The spaces between each structure allow mineralization to occur by surrounding biological fluids [2–5]. The fibrils are packed

in arrays and form fiber structures. The representative collagen structure with detailed their dimensions are given in Figure 2.2.

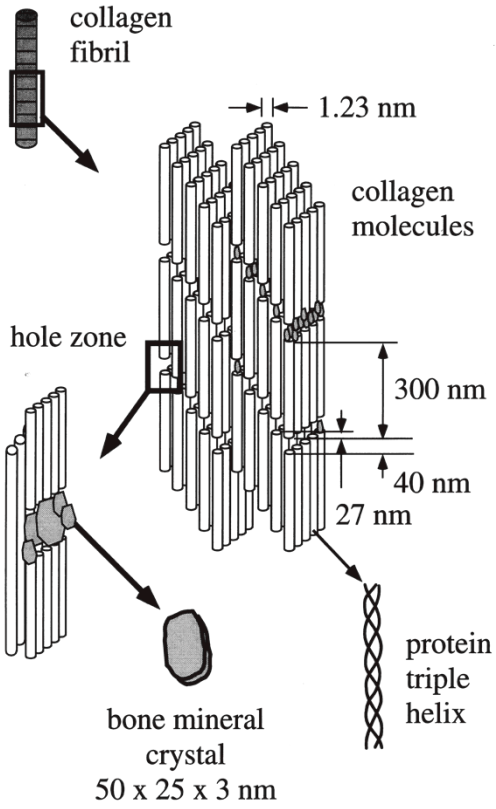

Figure 2.2 Schematic illustration of collagen fibrils, fibers and bone mineral crystals in nanoscale [5].

Mineral component of natural bone is comprised of nano-sized crystals of biological apatite, also called dahllite. The crystals have a plate-like shape having 50 nm of length, 25 nm of width and 1.5-4 nm of thickness [2]. The nanocrystalline bone apatite has significant amounts of impurities such as hydrogen phosphate (HPO_4), sodium (Na), magnesium (Mg), citrate $(C_6H_5O_7)^{4-}$, carbonate $(CO_3)^{2-}$, potassium (K) and other ions [5,6]. The first major function of mineral part of bone is acting as an ion source and regulating these ions' concentration. The second major function is that the combination of mineral part with the organic matrix components, basically

formation of composite structure, gives superior properties such as extremely high toughness and lightweight to bone [7,8].

The bone mineral differs from the stoichiometric form of hydroxyapatite (HAp; $Ca_{10}(PO_4)_6(OH)_2$) in terms stoichiometry (Ca/P ratio) because of the presence of trace ions and carbonate content, crystal size and morphology. HAp crystals as the mineral part of the bone are in calcium deficient and carbonated form with the stochiometry of Ca/P < 1.67 and the chemical formula of $Ca_{(10-x-y)}(HPO_4)_x(CO_3)_y(PO_4)_{(6-x-y)}(OH)_{(2-x-y)}$, $(0 < x,y < 1)$ [9].

Water is the third major component of bone. It is found within the fibers, between triple-helix structures, in the gaps, between fibrils and fibers and in the surface of bone mineral [2]. According to Wilson et al. [10], the water found at the surface at the bone mineral has two major functions. The water movements between bone mineral and collagen layer protect bone from deformation with less deformation and provides structural stability to bone. Secondly, movement of water protects collagen from shear under uniaxial stress, therefore, water, third major component of bone, preserves collagen from deformation.

Bone can recover and regenerate micro-scaled cracks and damages by itself. The Haversian channel found around the osteon, which are obtained from the collagen lamellar sheets, has an enormous reservoir of calcium and phosphate ions. By osteclasts and osteoblasts, monocrystalline apatite undergoes dynamic remodeling process [11]. However, bone cannot recover the fractures caused by trauma, tumor based removing operations or problems caused by aging. In these conditions, natural or synthetic bone graft materials are needed to use to heal the bone fractures.

2.2. Natural bone grafts

There are three types of natural bone grafts; xenografts, allografts and autografts. *Xenograft* is termed as transplanting graft from one species to another species. Unfortunately, xenografts have a high risk of viral infections, low osteogenicity, high immunogenicity and high resorption rate. These undesired situations make

xenograft usage limited [9]. One another type of graft type is *allografts* which are defined as transplant transferred from one member to another one of the same species. The drawbacks of allografts are similar to xenografts. Moreover, the risks of transmitting viral and bacterial infections, blood incompatibility are stronger compared to xenografts. When the tissue is taken from one site of the body and transplanted to another site in the same individual is defined as *autograft*. Autografts have the best results compared to other natural grafting methods because they are biocompatible, non-toxic and they have minimum risk of immunological problems, i.e. they do not cause any allergenic reactions. They support bone growth and contain osteogenic cell with bone matrix proteins. Usually, autografts are accepted by the body with no problem and integrated with the surrounding tissue easily [9,12]. However, the restricted donor sites limit the number of autografts, in addition, during the medical application, the trauma and scar formation of a donor tissue always occur.

These limitations of natural bone grafts give rise to development of various artificial materials as a usage of *synthetic bone grafts*. They are promising and widely studied because they can be modified according to specific applications [13]. Various metals, ceramics and polymers have been used as synthetic bone grafts in various biomedical applications such as bone implant, bone fracture repair and bone defect filling operations. The most important issue in the design of these materials is to provide the biocompatibility of the natural bone in terms of structural and mechanical properties. Metals and their alloys such as stainless steel, titanium alloys have been used as load-bearing materials because of their better mechanical properties. However, they do not show osteoconductivity (the ability to permit bone growth), osteoinductivity (the ability to stimulate the new bone formation) and osteointegration (the ability to chemically bond to the surface of bone without the combined fibrous tissue layer) [14]. Ceramic-based materials are the most promising for the irregular bone defect filling applications.

2.3. Synthetic bone grafts

2.3.1. Calcium sulfates

Calcium sulfates used as bone defect filling substitutes as a synthetic bone graft material. They were first used by Dreesman in 1892 as bone grafts for cavities due to bone defects. In 1950s and 1960s Peltier developed usage of calcium sulfates with extended clinical applications [15]. Generally calcium sulfates are not used as solid material, but they are used as a cement form. Calcium sulfate dihydrate (CSD) is obtained by mixing aqueous solution with calcium sulfate hemihydrate (CSH) via highly exothermic cement conversion reaction;

$$CaSO_4.{}^1/_2H2O + {}^3/_2H_2O \rightarrow CaSO_4.2H_2O \qquad \textit{Eq. [1]}$$

The CSD obtained from the reaction given in Equation 1 is a highly porous material with large surface area. It consists of interlocking needle-like crystals [16]. The porous microstructure of CSD cements allows the new bone tissue formation. However, the resorption rate of CSD is very high. For an ideal bone substitute material, the degradation rate should be similar to formation rate of new bone tissue. The resorption rate of CSD is faster than the formation of new bone; therefore, it is not desired situation for reconstruction of bone defect. In order to overcome this problem, calcium sulfate cements are used with other bone grafting materials [17].

2.3.2. Calcium phosphate ceramics

The chemical and structural similarity of calcium phosphates (CaP) to the mineral component of natural bone makes them promising candidates as bone substitute materials. Calcium ortophosphates are non-toxic, biocompatible and bioactive when interacting with bone tissue [18]. That's why they have been studied as bone repair materials for almost 90 years. Albee and Morrison firstly used tricalcium phosphate (TCP) as bone substitutes by *in vivo* implantation in 1920 [19]. In 1951, Ray [20] used hydroxyapatite (HAp) as an implantation substitute in rats and guinea pigs. After these experiments, other CaP compounds, but most commonly HAp, were

synthesized, characterized and used in different applications [21]. The list of different CaP compounds with their Ca/P molar ratio and other properties are given in Table 2.1.

Table 2.1 Calcium phosphates and their major properties [18]

Ca/P molar ratio	Compound	Formula	Solubility at 25°C, g/L	pH stability range in aqueous solutions at 25°C
0.5	Monocalcium phosphate monohydrate (MCPM)	$Ca(H_2PO_4)_2 \cdot H_2O$	~18	0.0-2.0
0.5	Monocalcium phosphate anhydrous (MCPA or MCP)	$Ca(H_2PO_4)_2$	~17	Stable at temperatures above 100°C
1.0	Dicalcium phosphate dihydrate (DCPD), mineral brushite	$CaHPO_4 \cdot 2H_2O$	~0.088	2.0-6.0
1.0	Dicalcium phosphate anhydrous (DCPA or DCP), mineral monetite	$CaHPO_4$	~0.048	Stable at temperatures above 100°C
1.33	Octacalcium phosphate (OCP)	$Ca_8(HPO_4)_2(PO_4)_4 \cdot 5H_2O$	~0.0081	5.5-7.0
1.5	α-Tricalcium phosphate (α-TCP)	$\alpha\text{-}Ca_3(PO_4)_2$	~0.0025	Not possible to precipitate from aqueous solutions
1.5	β-Tricalcium phosphate (β-TCP)	$\beta\text{-}Ca_3(PO_4)_2$	~0.0005	Not possible to precipitate from aqueous solutions
1.2-2.2	Amorphous calcium phosphate (ACP)	$Ca_xH_y(PO_4)_z \cdot nH_2O$, n=3-4.5; 15-20%$H_2O$	Not measured precisely	~5-12 (always metastable)
1.5-1.67	Calcium-deficient hydroxyapatite (CDHAp or CDHA)	$Ca_{10-x}(HPO_4)_x(PO_4)_{6-x}(OH)_{2-x}$ (0<x<1)	~0.0094	6.5-9.5
1.67	Hydroxyapatite (HAp or HA or OHAp)	$Ca_{10}(PO_4)_6(OH)_2$	~0.0003	9.5-12
1.67	Fluorapatite (FA or FAp)	$Ca_{10}(PO_4)_6F_2$	~0.0002	7-12
2.0	Tetracalcium phosphate (TTCP or TetCP), mineral hilgenstockite	$Ca_4(PO_4)_2O$	~0.0007	Not possible to precipitate from aqueous solutions

The most important property of CaP compounds is their solubility in aqueous solutions. Because if the solubility of a CaP is lower than the mineral part of bone, the degradation of CaP compound will be extremely slowly. On the other hand, if the solubility of a CaP compound is higher than that of mineral part of the bone, it will degrade [21]. Therefore, for the desired properties of application, a degradable or bioactive CaP is used. If the formation of new bone tissue is desired, a biodegradable CaP compound should be used. Figure 2.3 shows the solubility isotherms of CaP compounds in water.

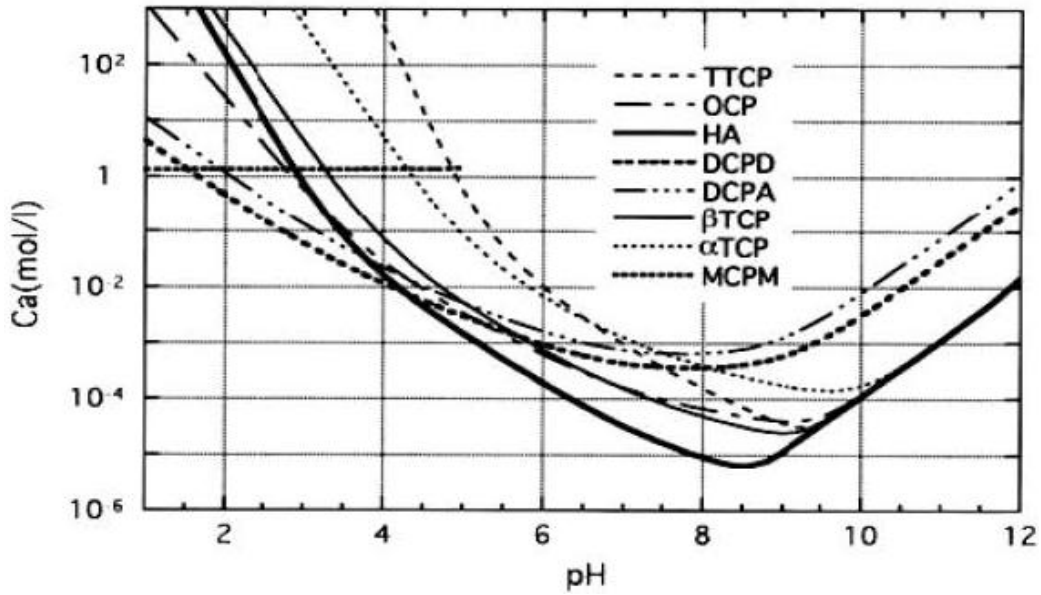

Figure 2.3 Solubility isotherms of different calcium phosphate compounds in water as a function of pH [22]

The solubilities shown in Figure 2.3 effect the *in vivo* performance of CaP compounds, the pH stability give information about the long-term use of the implants of CaP compounds.

Generally, the CaP compounds having Ca/P ratio in the range of 1-1.67 are only used for biomedical applications. Among the present CaPs listed in Table 2.1, those having Ca/P ratio less than 1 shows higher acidity and solubility (MCPM and MCPA), and those having Ca/P ratio higher than 1.67 shows higher basicity (TTCP). Because of these reasons, these CaP compounds are not suitable for implantation into body. However, they can be combined with other CaP compounds in order to make them suitable for biomedical applications [23]. Among different calcium phosphates listed in Table 2.1, HAp and TCP based compounds are the most suitable products for biomedical applications with bone-related ones.

2.3.2.1.1. Hydroxyapatite

In the 1980's the commercialization of the use of HAp in dental and surgical applications has occurred by the studies of Jarcho [24], De Groot [25] and Aoki [26]. Because of its similarity to mineral part of natural bone, HAp has been used for bone repair and bone regeneration application in different forms such as granules, blocks and scaffolds by itself. HAp has been also used with polymers or other ceramics as composites in orthopedic and dental applications mainly in non-load bearing parts due to their low mechanical properties [27].

Stoichometric HAp, $Ca_{10}(PO_4)_6(OH)_2$, is highly crystalline, the most biocompatible and the most stable when compared with other CaP compounds in aqueous solutions (as seen in Figure 2.3). Pure HAp crystallizes in the monoclinic space group. However above 250 °C, transformation from monoclinic to hexagonal phase occurs in HAp. Some impurities stabilize the hexagonal structure of HAp at room temperature. Because of this, natural HAp always exhibits hexagonal space group [28].

For the HAp preparation several techniques, basically divided into solid-state reactions and wet methods. In the case of the solid-state synthesis of pure HAp, other calcium phosphates react at temperatures above 1200 °C. Homogenous, crystalline and stoichiometric HAp can be obtained with this method. However, HAp synthesized from solid-state reactions is not similar with natural bone in terms of size and shape of the crystals. The wet method for preparation of HAp includes precipitation, hydrothermal, sol-gel and hydrolysis of other calcium phosphates. The product of wet methods is poorly crystalline, generally in non-stoichiometric form, resembling to calcium-deficient HAp (CDHAp) [29].

2.3.2.2. Calcium-deficient hydroxyapatite

CDHAp has the chemical formula of $Ca_{(10-x)}(HPO_4)(PO_4)_{(6-x)}(OH)_{(2-x)}$ where x changes between 0 and 1. It is in non-stoichiometric form, Ca/P ratio changes between 1.5 – 1.67. CDHAp is obtained by wet methods at pH>7 at low temperature

from different CaP compounds [21]. CDHAp nanocrystals show similar physico-chemical characteristics to bone mineral structures. Because of the deficiency of calcium and hydroxide ions, CDHAp nanocrystals have high solubility and high *in vivo* bioresorption rate [30]. It has relatively high surface area, so it exhibits high degradation rate. Therefore, CDHAp is a good candidate for temporary bone graft applications [31].

2.3.2.3. Tricalcium phosphate

There are three polymorphs of tricalcium phosphate (TCP); β-TCP, α-TCP and α′-TCP. Among them, α′-TCP is not practically used because it exhibits above 1430 °C and coverts instantaneously to α-TCP when cooling below the transition temperature. β-TCP is the room temperature stable phase and transforms to α-TCP at around 1125 °C. By effective quenching processes α-TCP can be preserved at room temperature.

α- and β-TCP are used in different clinical applications such as dental implants, maxillo-facial surgery applications and orthopedics. Although their chemical composition is same, their density and solubility is different from each other, which makes that their biological properties and clinical usage are different [32].

2.3.2.4. β-Tricalcium phosphate (β-TCP)

β-TCP (β-$Ca_3(PO_4)_2$) is the room temperature stable phase of TCP. β-TCP has been used clinically because of its osteoconductivity and tissue compatibility. As seen from Figure 2.3, HAp is the most stable compound in aqueous media, therefore HAp shows low degradation rates *in vivo* which makes it a best candidate material for long-term implants. In contrast, β-TCP is biodegradable, so it promotes new bone growth [33]. In the case of new bone growth, structure and the pore size of β-TCP is very critical [34]. β-TCP cannot be produced by precipitation from aqueous solutions. It can be prepared by thermal decomposition above 800 °C. Pure β-TCP is

used as polishing agents. Commonly, it is combined with other CaPs (mainly HAp) to form biphasic bioceramics and composites [29,32].

2.3.2.5. α-Tricalcium phosphate (α-TCP)

α-TCP (α-$Ca_3(PO_4)_2$) is the high temperature stable phase and it is obtained as metastable at room temperature. There are different methods to synthesis pure α-TCP. One technique is the thermal transformation of a CaP compound with Ca/P ratio of 1.5. CDHAp precursor, obtained from the precipitation of Ca and phosphate precursors with molar ratio of Ca/P = 1.5, can be thermally transformed into α-TCP by heating at 1250 °C for 2 h [35]. Bohner et al. [36] synthesized α-TCP from amorphous calcium phosphate (ACP) at much lower temperatures, i.e. 600 – 800 °C. The simplest and most direct method for obtaining α-TCP is heating β-TCP up to transformation temperature, ~1125 °C, and applying effective quenching [37].

The other technique for producing pure α-TCP is the solid-state reaction of calcium and phosphate precursor. The commonly used precursors are $CaCO_3$: $CaHPO_4$, $CaCO_3$: $NH_4H_2PO_4$ and $CaCO_3$: $Ca_2P_2O_7$. These solid precursors are milled together in order to mix them well, reduce the surface area, therefore, increase the contact area. After milling, mixed precursors are fired at a temperature between 1200 – 1500 °C for 2 – 48 h. Finally, effective quenching should be applied in order to obtain only α-TCP phase without forming any other phases [32].

Although α-TCP and β-TCP have the same chemical composition, the most important difference between them is that α-TCP is much more soluble than β-TCP. This property of α-TCP makes it the major component of apatitic calcium phosphate cement. α-TCP is converted to HAp in an aqueous solution with the reaction given in Equation 2. The end product of this conversion is a hardened solid mass in a cement form [21,32].

$$3\ \alpha\text{-}Ca_3(PO_4)_2 + H_2O \rightarrow Ca_9HPO_4(PO_4)_5(OH) \qquad \textit{Eq. [2]}$$

2.4. Bone cements

Bone cements are used for filling irregular shaped bone defects. They are self-setting and injectable systems. One or more solid phase is mixed with liquid phase. Firstly it forms a viscous paste and transforms into a solid and hardened mass. There are various important properties of bone cements. Firstly, setting time of bone cement is critical. Bone cements must set slowly to give enough time for implantation but must be fast not to delay the operation. For dental applications, setting time should be close to 3 min and for orthopedic applications it should be close to 8 min. But it must be lower than 15 min for any cases [38]. The degradation rate of bone cements is also very important. It should degrade after natural bone tissue formation in order to be not harmful for bone healing. Moreover, it should have some amount of macroporosity for tissue ingrowth [39].

Firstly, polymethylmethacrylate (PMMA) has been used as bone cement. It was firstly introduced by Charnley and Smith in the early 1960s [40]. Hardened PMMA cement is obtained by the polymerization reaction of MMA monomer. However, its clinical use is limited because of several problems. It is a bioinert material, therefore, there is an insufficient linkage to bone surface. The polymerization reaction of PMMA is highly exothermic which results in increasing the temperature up to 120 °C and deformation to surrounding tissue [41]. Moreover, release of unreacted toxic MMA monomer poses a risk of chemical necrosis of bone [42]. Mechanical properties of PMMA cements are also problematic; they are brittle and have a poor fatigue life [43]. Because of the given problems of PMMA cements, more promising candidates, which are bioactive and bioresorbable, are investigated.

2.4.1. Calcium phosphate bone cements

Calcium phosphate cements (CPC) were first studied by LeGeros et al. [44] and Brown and Chow [45] in the early 1980s. Brown and Chow formed an apatitic bone cement by mixing tetracalcium phosphate and dicalcium phosphate with an aqueous

solution at physiological conditions. In 1987, Lemaitre et al. [46] formulated brushite cement consisting of β-TCP and monocalcium phosphate monohydrate or phosphoric acid [27].

CPCs are formed by mixing one or more calcium phosphate powders with aqueous solution. Firstly, a viscous paste is formed and then it turns into hardened solid mass in a few minutes. Setting reactions occur by dissolving calcium phosphates and precipitation into crystals of cement end product [47].

There are various combinations of CaP compounds which set into solid and hardened products upon mixing with liquid reactant. According to the solubility data, depending on the pH value of cement, there are only two end products are possible; brushite when pH<4.2 and precipitated poorly crystalline apatite when pH>4.2. The final hardened product is very critical because it determines the solubility, therefore, bioresorbability. Since the mineral part of the natural bone is similar to apatite with ion substitutions, apatite cements have been studied in detail.

2.4.1.1. Brushite cements

The major end product of brushite cements is dicalcium phosphate dihydrate (DCPD, $CaHPO_4 \cdot 2H_2O$). Brushite cements are obtained only by acid-base interaction. β-TCP + MCPM [46], β-TCP + H_3PO_4 [48] and TTCP + MCPM + CaO [49] are some formulations for setting of brushite cements [47]. Since the precipitation of brushite cements occurs when the pH is lower than 6, the setting of the paste of brushite cements are acidic [48].

The solubility of brushite cement depends on the basicity. The solubility decreases with increasing the amount of basic CaP compounds. The setting reaction of cements is related with the dissolution of initial compounds. Therefore, the setting time of brushite cements depends on the solubility of basic phases; the higher the solubility of basic phase, the shorter the setting time.

Brushite is biocompatible and bioresorbable. When compared with apatite, brushite has higher solubility, seen in Figure 2.3. Moreover, it is metastable under physiological conditions. Because of higher solubility and metastability, brushite cements' degradation rate is higher than apatite cements'. Therefore, they quickly degrade *in vivo*, this cause rapid decrease in strength [50]. DCPD partially transforms to CDHAp by the given reaction in Equation 3;

$$(10\text{-}x)CaHPO_2{\cdot}2H_2O \rightarrow Ca_{(10-x)}(HPO_4)_x(PO_4)_{(6-x)}(OH) + (4\text{-}x)H_3PO_4 + (18\text{-}x)H_2O \quad \textit{Eq. [3]}$$

Due to the transformation from DCPD to CDHAp, release of orthophosphoric acid may cause tissue inflammation [47]. In addition to tissue inflammation due to the acidic environment, short setting times and low mechanical properties of brushite cements hinder their broader clinical usage.

2.4.1.2. Apatite Cements

The end product of setting reaction of apatite cement is poorly crystalline HAp or CDHAp. Trace amount of the unreacted initial CaP compounds can also be present. The end product of poorly crystalline CDHAp has similar characteristics with mineral part of the natural bone. There are two types of setting reaction of apatite cements; mixing more than one CaP compounds and hydrolysis of one metastable CaP compound with the same Ca/P ratio with the end product of apatite cement, CDHAp [47].

The first cement formulation is set by the acid-base interaction, which means that relatively acidic CaP compound mixes with relatively basic CaP compound in an aqueous media to form a neutral hardened CaP solid mass. Brown and Chow [45] was reported the first cement by reaction between TTCP (basic) and DCPA (acidic) in an aqueous media shown in Equation 4 and 5.

$$2\ Ca_4(PO_4)_2O + 2\ CaHPO_4 \xrightarrow{H_2O} Ca_{10}(PO_4)_6(OH)_2 \quad \textit{Eq. [4]}$$

$$6\ Ca_4(PO_4)_2O + 3\ CaHPO_4 \xrightarrow{H_2O} 2\ Ca_9(HPO_4)(PO_4)_5OH \qquad \textit{Eq. [5]}$$

As seen from Equation 4 and 5, by changing the ratio of TTCP and DCPA, both stoichiometric HAp and CDHAp can be obtained. When TTCP and DCPA are dissolved in aqueous media, Ca^{2+} and $(PO_4)^{3-}$ ions are released. HAp formation takes place when sufficient amounts of ions are supplied. With the given two equations it is seen that the TTCP with Ca/P ratio of 2 dissolves more calcium ions. Therefore, cement setting rate is determined by the dissolution of $(PO_4)^{3-}$ from DCPA. The setting time of apatite is longer than brushite cements. Setting time of TTCP + DCPA in DI water was reported approximately 30 minutes which is not suitable for clinical use [27]. For decreasing the setting time of cement, Ishikawa et al. [51] reported that using hydrogen phosphate aqueous solution supplies phosphate ions, therefore, this increases the setting rate of cement.

The second type of CPC setting reaction is hydrolysis of a metastable CaP compound. The reactant compound and end product have the same Ca/P ratio. In this category, the most popular self-setting single compound is α-TCP which is also the focus of this study. α-TCP cements were firstly studied by Monma and Kazanawa in 1976 [52]. The setting reaction of α-TCP cement is given in Equation 6;

$$3\ \alpha\text{-}Ca_3(PO_4)_2 + H_2O \rightarrow Ca_9(HPO_4)(PO_4)_5OH \qquad \textit{Eq. [6]}$$

Cement reaction of α-TCP occurs in two stages; first dissolution of α-TCP precursor in aqueous solution and then precipitation of CDHAp by nucleation and growth.

The cement-type reaction kinetics of α-TCP depends on temperature, chemistry, crystallinity and particle size of α-TCP powders [47]. The setting reaction of α-TCP to CDHAp consists of three stages, (1) dissolution of α-TCP powders in aqueous solution, (2) nucleation and (3) growth of crystals. Therefore, the setting reaction can be changed by modifying these stages. Dissolution of α-TCP powders starts from the

surface, so increasing the surface area between powder and liquid results in faster reaction kinetics. The easiest way to increase the surface area of powders is performing long milling operations [53]. However, by milling operation the particles can not be decreased than a few micrometers [54]. Synthesizing nanosized α-TCP powders can be another way for increasing the surface area. By decreasing the pH of reactant media using Na_2HPO_4 can also increase the dissolution rate [53]. In order to increase the nucleation rate of CDHAp crystals, the desired end product is seeded. This improves the reactivity and increases the reaction rate. Brown and Chow [45] was reported that seeding 25 % of HAp to DCPD-TTCP system reduced the setting time by 50 %. Similar situation is also valid for α-TCP, in this case HAp which acts as nucleation agent was seeded. Durucan and Brown [55] showed that seeding 1 – 5 wt. % HAp accelerates the hydration reaction rate and decreases the time required for both nucleation and growth. Using a liquid phase with dissolved calcium and phosphate ions increases both the nucleation and growth rate. This phenomena is called as common ion effect [53].

2.5. Therapeutic agents incorporation in calcium phosphate cements

CPCs are injectable, biodegradable materials, they set at ambient temperatures and they have near neutral pHs with high surface area. Therefore, these properties make these cements promising candidates as drugs, hormones, proteins, growth factors and metallic ion carriers.

2.5.1. Calcium phosphate cements as drug delivery systems

CPCs can be used for as drug delivery systems for the treatment of various skeletal diseases, such as bone tumors, bone osteoporosis and osteomyelitis. These treatments normally require long and painful therapies [56]. The drugs can be introduced into both the liquid or solid phase of the cements. During the chemical reaction and the setting of cements, physicochemical properties of drugs should not change. After setting, the drugs should be slowly released from the pores of cements. Figure 2.4 shows the incorporation of drugs in cement systems [56,57].

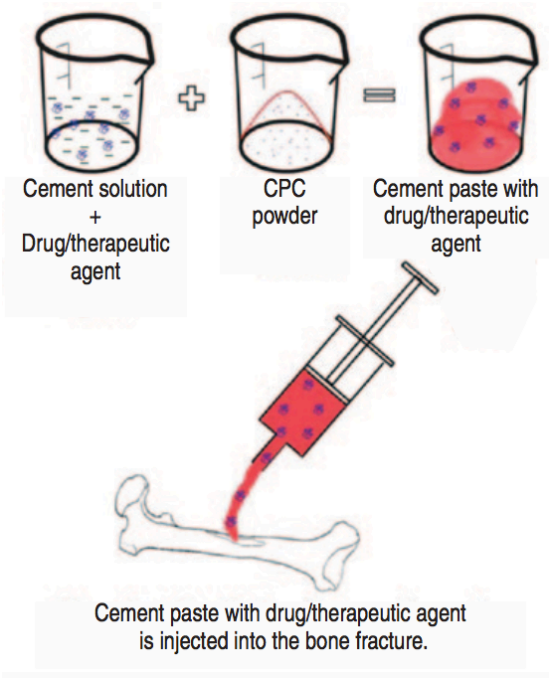

Figure 2.4 Schematic illustration of preparing drug incorporated CPCs and its application into a bone fracture

Different types of drugs such as antibiotics, anti-cancer drugs, anti-inflammatory drugs have been incorporated to CPCs for various applications.

In bone replacement, after surgical therapy, in the presence of orthopedic infections, in periodontal diseases antibiotics are used for treatment. The most important key factor for the success during the surgical intervention of implantation is the preventation from bacterial infections. Wound contamination or infections occurred after operation may cause some problems. Therefore, antibiotics are often provided either orally or intravenously. However, little accessibility of the site of injection extends the treatment of bone infections. Therefore, some treatments are developed, such as doping antibiotics to PMMA, calcium sulfate or calcium phosphate ceramics. However, these treatments have some disadvantages. In order to overcome these drawbacks, antibiotics are combined with CPCs. Antibiotics are the most extensively studied drugs for incorporation to CPCs. By the addition of antibiotics, the setting reaction of CPCs can be modified, as a result, the physico-chemical and

mechanical properties can change. Commonly, antibiotics tend to increase the setting time and decrease the mechanical strength of CPCs. Takechi et al. [58] incorporated different concentrations of flomoxef sodium, which is a widely used antibiotic, to the solid phase of an apatitic cement. They reported that by increasing the concentration of antibiotics, the mechanical strength of cement was decreased. This decrease was attributed to increased porosity and to some inhibition of the setting reaction. After 72 h 55-60 % of antibiotic was released from the cement. Ratier et al. [59] reported that the reduction in mechanical properties of cements is because of the chemical interaction between antibiotic and the cement. When the antibiotics were introduced to the cement systems already complexed with calcium ions, the interaction between cement and antibiotics were limited. Therefore, the setting time and mechanical strength were not influenced with addition of higher amounts of antibiotics [60].

Not only antibiotics, but also as anti-inflammatory, analgesic and anti-cancer drugs are incorporated to CPCs for different applications in the musculoskeletal system. Ginebra et al. [61] studied the effect of addition of amino salicylic acid, which is an analgesic and anti-inflammatory drug, to an α-TCP based cement. With the incorporation of drug, the injectability was improved, mechanical strength increased. However, the reaction rate of cement decreased. As an anti-cancer drug mercaptopurine, which inhibits the proliferation of tumoral cells, was studied by Otsuka et al. [62]. They incorporated it to CPC. They reported that setting reaction was not affected with drug incorporation. Moreover, they observed that by changing the liquid-to-powder ratio of cement paste the drug release rate can be modified [60].

2.5.2. Incorporation of metallic ion in calcium phosphate cements

Commonly used organic drugs are not suitable for the fabrication of porous scaffold with desired structural and mechanical properties. The fabrication conditions such as high temperature, use of pressure and free radicals are not compatible with drug stability and drug release. This fabrication processes lead to decomposition of drugs. Therefore, the use of metallic ions become attractive as therapeutic agents as they

are more stable and they do not have a risk of decomposition [63]. Moreover, metallic ions interact with other ions and bind to macromolecules such as enzymes and nucleic acids so they can modify cellular and biological functions and cell metabolism [64]. All these properties are related with the kinetics of release of metallic ions from scaffold material. However, concentration of metallic ion loading and controlled release of these ions are very important for delivery of metallic ions for therapeutic use. Higher concentration of metallic ion and extensive release of ions can cause toxicity [63].

Calcium phosphates ceramics and calcium phosphate cements are attractive materials for doping metallic ions. Therefore, there are numerous of works related to different metallic ions, as therapeutic agents, doped to both various CaP ceramics and cements. Among these ions, Cu^{2+} and Ag^{+} are used as antibacterial agents, Sr^{2+}, Mg^{2+}, Zn^{2+} and Si^{4+} are used to enhance bone growth and reduce bone resorption and Se-based ions (SeO_4^{2-} and SeO_3^{2-}) are used as anti-cancer agents.

2.5.2.1. Metallic ion dopants for bone formation

Strontium is a present ion in bone and it is known that low doses of Sr are used for osteoporosis treatment. Strontium in the form of Sr chloride or Sr ranelate promotes bone formation and reduces bone resorption [65], [66]. The positive effects of Sr in long-term clinical use make them promising candidates as doping agents for CaPs. The effect of Sr^{2+} ion in both brushite and apatite cements were investigated. It was reported that Sr addition retards the setting reaction; on the other hand, the mechanical properties of brushite cements are not significantly influenced by the Sr incorporation [67]. The hydrolysis reaction rate of α-TCP decreased with the addition of Sr. The low doses of Sr usage allows to modulate the setting time of cement and it has a beneficial effect on bone cells. Therefore, Sr-incorporated α-TCP based cements are potential candidates in the treatment of osteoporosis [68].

Silicon is a necessary trace mineral for the bone formation, it increases the density of bone, so the bone strength is enhanced [69]. Si addition improves the bioactivity of

CaPs therefore, Si-incorporated CaP have been widely studied. During Si incorporation in CaPs, SiO_4^{4-} is substituted for PO_4^{3-} groups. There are numerous studies on the Si-doped HAp systems. However, there are few studies related with the Si-substitution in α-TCP powders and CPCs [70]. Wei and Akinc [71] studied on doping Si and Zn in TCPs with the molar ratio (Zn+Ca)/(P+Si) of 1.5. They found that Zn-incorporation favors the formation of β-TCP, while Si doping favors the formation of α-TCP. Reid et al. [70] prepared Si-substituted CaP powders with the constant Ca/(P+Si) ratio of 1.5. They showed that single phase Si-incorporated α-TCP (Si-α-TCP) forms when the Si content is between 0.59-1.14 wt. %. When it is below than 0.59 wt. %, there phase mixtures of Si-α-TCP, β-TCP and HAp forms. When Si content is higher than 1.14 wt. % Si-α-TCP and HAp mixture forms. There are limited studies on the Si incorporated α-TCP cements in literature.

Mg and Zn ions are known to influence osteoclast and osteoblast activity; therefore, they promote bone formation. The effect of Mg and Zn ions on CPCs was investigated with preparing cement by mixing Mg and Zn doped amorphous calcium carbonate phosphate with α-TCP and monocalcium phosphate monohydrate. It was seen that setting time and porosity decreases with the order of Mg > Zn, whereas the order is reversed for compressive strength [72].

2.5.2.2. Metallic ion dopants as anti-bacterial agents

Silver has been used as antibacterial agent in medicine for a long time, it is used in ionic form or particulate form for various applications. Ag^+ prevents biofilm growth onto surfaces of materials and inhibits bacterial proliferation by the release of silver ions in controlled manner [73]. Moreover, Ag^+ binds with microbial DNA of –SH groups of bacteria enzymes. This bonding makes the bacteria cells inactive [74]. Therefore, Ag-doped calcium phosphates have been widely studied. Ewald et al. [75] produced silver-doped apatite and brushite cements using silver-doped α-TCP and silver-doped β-TCP respectively. It was reported that low doses of Ag^+ usage allows host cells to grow without exhibiting any toxic properties and growth of bacteria

cells are inhibited. Moreover it was reported that the compressive strength of silver-doped brushite cement was increased by 30 %, whereas that of silver-doped apatite cement was reduced by 50 %. However, this decrease is acceptable for the use in the craniofacial region. Peetsch et al [76] paid attention that using higher concentration of silver cause occurrence of toxic reaction for the surrounding tissue. Without reaching the cytotoxic silver concentration, using silver-doped CPCs can achieve antibacterial effect.

2.5.2.3. Selenium: Anti-cancerous metallic ion dopant

Selenium is a necessary mineral for human biology and it's a component of selenoproteins, which are essential to human immune systems and have important enzymic functions. Selenium is an important ion for human health in terms of cancer preventation [77]. The dose of selenium supplemented is highly important for protective roles against cancer cells. Food and Agriculture Organization/World Health Organization has set the recommended daily dose of selenium 26-34 μg/day, higher than this level is required to inhibit genetic damage and cancer development. The advised doses of selenium for cancer treatment are 100-200 μg/day and approximately 400 μg Se/day is considered an upper safe limit [78].

Selenium and its compounds have been widely used as coating material and dopant as anti-cancer agent. Wang et al. [79] synthesized selenium-incorporated HAp. They reported that Se addition activates the apoptosis of cancerous bone cells and this effect is suggested to activate intrinsic mitochondrial apoptotic pathway. Selenium incorporation in CPC has not been studied yet.

2.6. Objective and structure of the thesis

There are two main objectives of this thesis. The first objective is synthesis of phase pure and reactive α-TCP by solid-state reaction of calcium and phosphate precursors and investigating the hydration kinetics of convertion of α-TCP into hardened CDHAp by cement reaction. The second main objective is producing Se-

incorporated α-TCP (α-TCP:Se) by again solid-state reaction with additionally using selenite precursor. α-TCP:Se is hydrated at 37 °C to obtain hardened CDHAp:Se cement product. The structural characterization and reaction kinetics are examined in a comparative manner.

The thesis is mainly composed of two chapters. Chapter 3 gives the experimental protocols and analytical techniques used in the thesis in detail. In Chapter 4 results on pure and Se-incorporated α-TCP (α-TCP:Se) powders synthesized by solid-state reaction are shown. The changes in chemical, morphological and structural properties of α-TCP were investigated with different amounts of Se-incorporation. α-TCP and α-TCP:Se powders were hydrated with DI water at 37 °C and the reaction kinetics of conversion reaction to hardened CDHAp cement product were investigated. The hydration efficiency with different amounts of Se incorporation was compared with pure α-TCP. Phase identification, morphological and chemical investigation of hydration products of α-TCP and α-TCP:Se was performed.

CHAPTER 3

MATERIALS AND METHODS

The α-tricalcium phosphate (α-$Ca_3(PO_4)_2$ or α-TCP) and Se-incorporated α-TCP (α-TCP:Se) powders were synthesized by a high temperature solid-state reaction of proper starting materials. In this chapter, experimental procedure of the synthesis of α-TCP and Se-incorporation to α-TCP were described. Assessment of cement type conversion efficiency of pure and Se-incorporated α-TCP → CDHAp is described. Material characterization techniques used in this thesis and analyses details were explained in this chapter.

3.1. Materials

α-TCP was prepared by a high temperature solid-state reaction of stoichiometric amounts of calcium carbonate ($CaCO_3$, reagent grade Merck, Germany) and chemically synthesized monetite ($CaHPO_4$) at 1200 °C for 2 h. Monetite was synthesized by using calcium precursor of $CaCO_3$ and phosphorous source of phosphoric acid (H_3PO_4, 85wt. %, Merck, Germany). For Se-incorporated α-TCP as a Se source sodium selenite (Na_2SeO_3, Bioreagent, suitable for cell culturei 98 %; Sigma-Aldrich) was used. Ultrapure deionized (DI) water was used.

3.2. Experimental Procedures

3.2.1. Synthesis of pure α-TCP

For the synthesis of pure α-TCP, one of the precursor was chemically synthesized $CaHPO_4$, which was started from $CaCO_3$. First 15 g of $CaCO_3$ was calcined at 1010 °C for 2 h. After that reaction, the product was CaO. 10.9 g of CaO was hydrated with 100 mL excess DI water at room temperature for approximately 1 h to obtain the slurry of $Ca(OH)_2$. Then, the slurry was mixed with 22.4 g phosphoric acid at

around 55-60 °C for 1.5 h. This reaction was done in open atmosphere by heating the mixture on a hot plate under continuous mixing. $CaHPO_4$ was precipitated in the aqueous mixture. After, the mixture was vacuum filtered with a fine filter paper. The solid product was kept at 70 °C overnight for drying.

α-TCP was synthesized by a high temperature solid-state reaction of $CaCO_3$ and $CaHPO_4$ with a reaction given in Equation 7:

$$CaCO_{3(s)} + 2CaHPO_{4(s)} \rightarrow Ca_3(PO_4)_{2(s)} + H_2O_{(g)} + CO_{2(g)} \quad \textit{Eq. [7]}$$

1:2 mol proportion of $CaCO_3$ and $CaHPO_4$ was mixed in a Nalgene^{TM} container with liquid medium, which is acetone in this experiment, and mixed by Turbula mixer (Model T2F, System Schatz, Switzerland). For evaporating acetone from the mixture, the homogenized mixture was dried in air for overnight, then it was fired at 1200 °C for 2 h in alumina crucible to obtain α-TCP.

There are two most commonly observed polymorphs of TCP, which are α- and β-TCP. α-TCP is high temperature polymorph and it transforms into β-TCP at 1150 °C under equilibrium cooling conditions. Therefore, in order to avoid formation of β-TCP and obtain phase pure α-TCP, effective quenching is required. After firing the $CaCO_3$ and $CaHPO_4$ mixture at 1200 °C for 2 h, the fired red hot mass was immediately quenched in air using stainless steel plate. Firstly, the quenched product was ground using mortar and pestle into powder form then α-TCP powders were milled in a Nalgene^{TM} in liquid medium of acetone for 1 h with 20 mm zirconia balls by Turbula mixer (Model T2F, System Schatz, Switzerland).

3.2.2. Synthesis of Se-incorporated α-TCP

For the synthesis of Selenium-incorporated α-TCP (α-TCP:Se), Se ion was not incorporated directly to α-TCP powder during high temperature reaction. Se incorporation was performed with modifying the chemistry of the custom synthesized precursor used in obtaining the α-TCP, which is monetite, $CaHPO_4$.

Pure 15 g of $CaCO_3$ was calcined at 1010 °C for 2 h. The reaction product CaO was mixed with 100 mL excess DI water to obtain $Ca(OH)_2$ in slurry form.

For Se-incorporation Na_2SeO_3, a Se containing salt was used as a Se ion source. For 5 wt. % Se-incorporated $CaHPO_4$ ($CaHPO_4$:Se:5wt.%), 3 g of Na_2SeO_3, for 10 wt. % Se-incorporated $CaHPO_4$ ($CaHPO_4$:Se:10wt.%) 6.1 g of Na_2SeO_3 was used.

$Ca(OH)_2$, different amount of Na_2SeO_3 and proper amount of H_3PO_4 was mixed at 55-60 °C for 1.5 h. $CaHPO_4$:Se was precipitated in the aqueous mixture. After, the mixture was vacuum filtered with a fine filter paper. The solid product was kept at 70 °C overnight for drying. Figure 3.1 shows the schematic illustration of synthesis route of modified monetite powders.

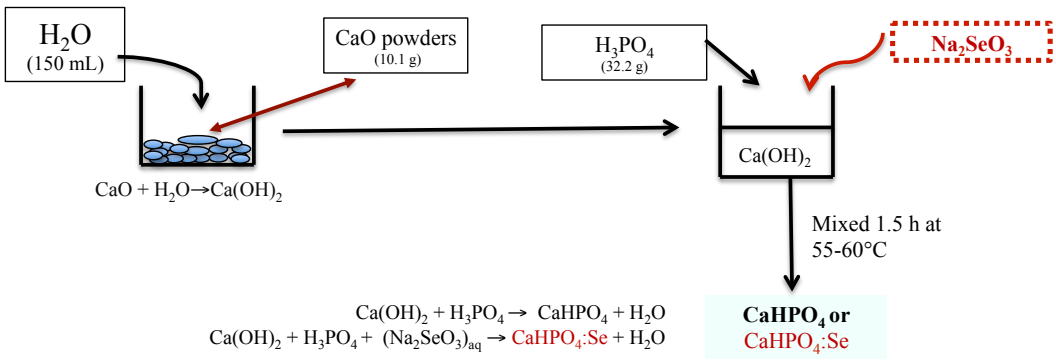

Figure 3.1 Schematic illustration of synthesis of pure $CaHPO_4$ and Se-incorporated $CaHPO_4$

Se-incorporated α-TCP (α-TCP:Se) was synthesized by a high temperature solid-state reaction of $CaCO_3$ and $CaHPO_4$:Se with a reaction given in Equation 8:

$$CaCO_{3(s)} + 2CaHPO_4{:}Se_{(s)} \rightarrow Ca_3(PO_4)_2{:}Se_{(s)} + H_2O_{(g)} + CO_{2(g)} \quad \textit{Eq. [8]}$$

1:2 mol proportion of $CaCO_3$ and $CaHPO_4$:Se was mixed in a Nalgene^{TM} container with acetone and mixed by Turbula mixer (Model T2F, System Schatz, Switzerland). For evaporating acetone from the mixture, the homogenized mixture was dried in air for overnight, then it was fired at 1200 °C for 2 h in alumina crucible to obtain α-TCP:Se. The synthesis of α-TCP from $CaHPO_4$ is shown in Figure 3.2.

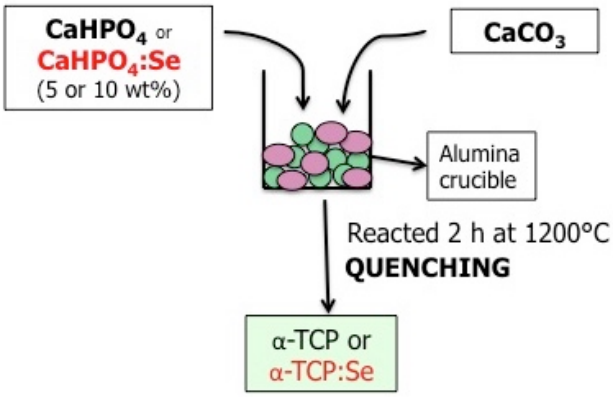

Figure 3.2 Schematic illustration of synthesis of pure α-TCP and Se-incorporated α-TCP

The complete characterization of $CaHPO_4$:Se and α-TCP:Se will be given in the Results chapter. Figure 3.3 shows the flowchart of the solid-state synthesis route of pure and Se-incorporated α-TCP particles.

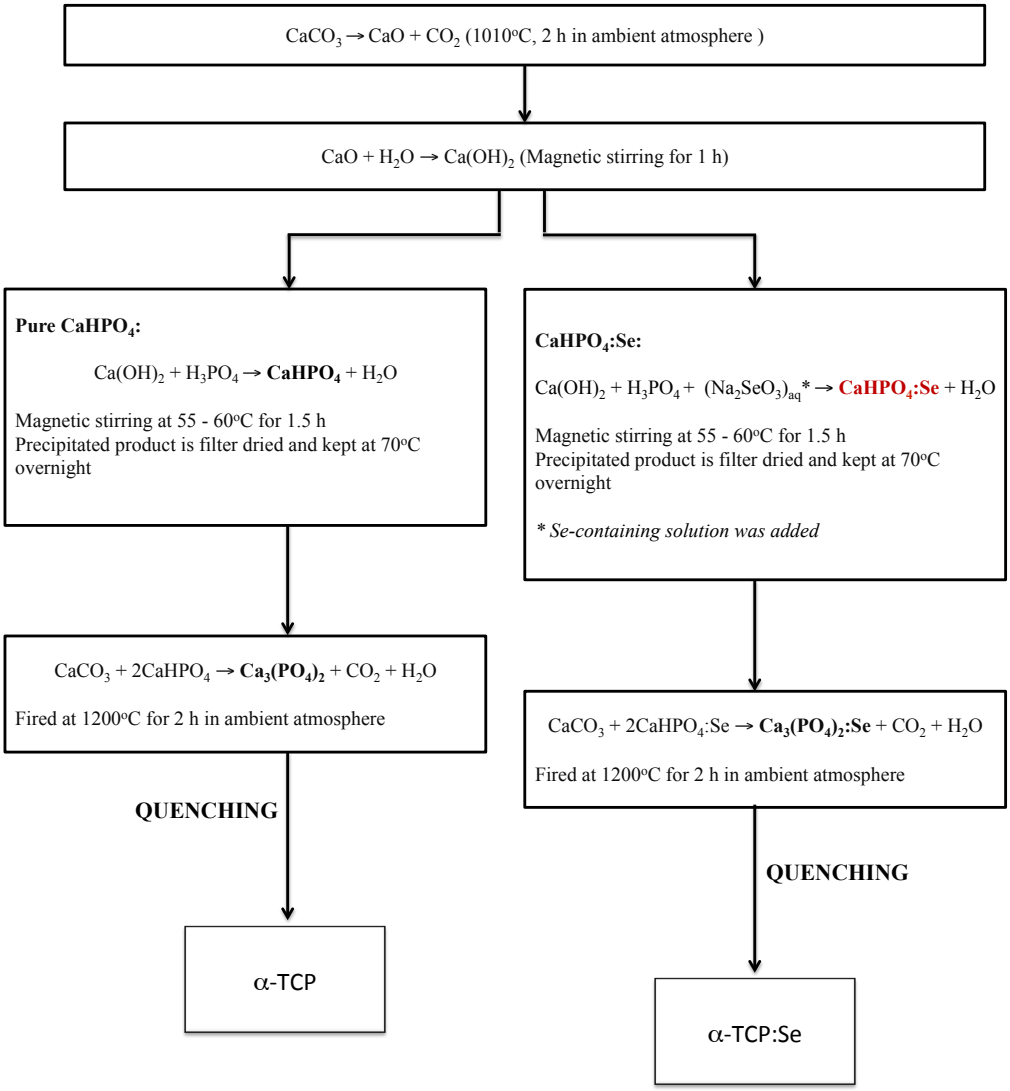

Figure 3.3 Flowchart of the solid-state synthesis of pure α-TCP and Se-incorporated α-TCP

3.2.3. Preperation of pure Calcium-Deficient Hydroxyapatite (CDHAp) and Se-incorporated CDHAp (CDHAp:Se) cements

For the preparation of pure CDHAp, pure solid-state reaction products of α-TCP powders were reacted with DI water to obtain the final form of cement. Firstly, the α-TCP powders were placed in glass flasks and required amount of DI water was

ejected on the flasks for starting the reaction between α-TCP powders and DI water. The reaction was conducted in a closed bath system at 37 °C for 48 h. After the cement-type conversion reaction was completed, α-TCP powders were completely transformed to CDHAp cements with a reaction given in Equation 9:

$$3\alpha\text{-}Ca_3(PO_4)_2 + H_2O \rightarrow Ca_9(HPO_4)(PO_4)_5(OH) \qquad \textit{Eq. [9]}$$

The Se-incorporated CDHAp cements were prepared by mixing as-synthesized α-TCP:Se powders and adequate amount of DI water with solid:liquid ratio of 1:2 in glass flask. The mixture was kept in closed bath system at 37 °C. The production processes of pure and Se-incorporated CDHAp cements are schematized in Figure 3.4. Reaction kinetics of hydration of α-TCP powders was investigated with isothermal calorimetry which will be given in Results chapter.

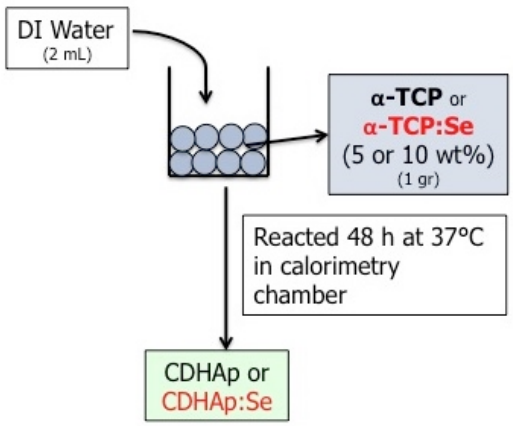

Figure 3.4 Schematic illustration of synthesis of pure CDHAp and Se-incorporated CDHAp

3.3. Characterization of solid state synthesis products of α-TCP and α-TCP:Se and their hydrated cement-end products

3.3.1. Phase Identification: X-Ray Diffraction Analysis

Phase identifications and formation of unwanted secondary phases investigations for α-TCP and α-TCP:Se particles, their precursor powders which are $CaHPO_4$ and $CaHPO_4$:Se and their hydration products which are CDHAp and CDHAp:Se were performed by X-Ray Diffraction (XRD) measurements using Bruker D8 Advance diffractometer. XRD pattern was obtained using Cu $K\alpha$ radiaton with λ: 1.5418 Å, at an operation voltage of 40 kV and the current of 30 mA. The XRD patterns of all calcium phosphate powders and their cement-type hydration products were scanned between 2θs of 20°-40° at a scanning rate of 2°/min.

3.3.2. Microstructural Investigation: Scanning Electron Microscopy

The microstructure of pure and Se-incorporated calcium phosphate powders, TCP particles and their cement products were investigated in terms of particle shape, size and size distribution using FESEM Nova NanoSEM 430 model scanning electron microscope (SEM). Since all the powders are not conductive, they were coated with gold before the SEM examination.

3.3.3. Energy Dispersive X-Ray Analysis

In order to identify the composition of component elements, Energy dispersive X-Ray analysis (EDS) was performed using EDS detector in JEOL 2100 F model (JEOL Ltd,, Tokyo, Japan). The EDS spectrum was collected at 20 kV for 60-70 seconds. Carbon and oxygen atoms were excluded from the EDS spectrum results because of their low reliability for EDS analysis. For each samples the wt. % of each element was finally listed.

3.3.4. Chemical Structure Analysis: Infrared Spectroscopy

Fourier transform infrared spectroscopy (FTIR) analyses were performed to investigate the chemical structure of pure and Se-incorporated α-TCP powders and their hydrated cement-type products, CDHAp. The analyses were done using FTIR Frontier spectrometer (Perkin Elmer, USA). The samples were investigated in pellet form. They were prepared by mixing 3 mg of investigated powders with 200 mg KBr powders. The mixture was ground using agate mortar and pestle and filled into a pellet forming die. The pellets were obtained after applying approximately 7 tons of force for 40 seconds. The spectrum was collected in absorbance mode between 2000-450 cm^{-1}.

3.3.5. Reaction Kinetics Studies: Isothermal Calorimetry

The hydration reaction kinetics of α-TCP and α-TCP:Se particles was studied using isothermal calorimetry (TAM Air TA Instruments, Lindon, USA). The powder was placed in a glass ampule and a liquid reactant, which is DI water in this study, was filled in a syringe. The glass ampule with syringe was inserted into a closed calorimetry chamber. The solid:liquid ration was 1:2 for all experiments. Meanwhile, as a reference sample appropriate amount of inert $CaSO_4.½H_20$ powder was placed in a different ampule and inserted into the reference chamber. Baseline was obtained until the thermal equilibrium was established. After that, DI water was injected into the powder sample. With mixing DI water and reactant powder, the cement reaction was started. The isothermal chamber was kept at physiological temperature (37 °C) for all experiments. The rate of heat release (dQ/dt) was continuously monitored during the reaction. Finally, the heat flow due to hydration as a function of time was obtained which was related to reaction kinetics and hydration efficiency.

CHAPTER 4

RESULTS AND DISCUSSION

In this chapter, characterization of pure α-TCP and different amounts of Se incorporated α-TCP powders synthesized by solid-state reaction that was explained in Section 3.2.1 and Section 3.2.2 is presented with a comparative manner. First of all, in order to analyze the phases and their characteristics XRD was performed for α-TCP and α-TCP:Se powders. The effect of Se incorporation in the phase characteristics and crystallinity was investigated. The chemical identity of the powders was examined by SEM-EDS analyses. The microstructural/morphological properties and the extent and effect of Se incorporation were studied by SEM analyses. Further, chemical identification was performed by FTIR analyses for both α-TCP and α-TCP:Se powders. Cement-type reaction kinetics was investigated by isothermal calorimetry for α-TCP and α-TCP:Se powders in a comparative manner. The cement-end products of CDHAp and CDHAp:Se was revealed by SEM, XRD, EDS and FTIR. The effect of the addition of Se in reaction kinetics was examined in detail.

4.1. Characterization of α-TCP and α-TCP:Se powders

Selenium incorporation was performed by modifying the chemistry of one of the custom synthesized precursor phase used in obtaining α-TCP rather than performing during direct high temperature synthesis of α-TCP. Figure 4.1 shows the XRD pattern of pure, 5 wt. % and 10 wt. % Se-incorporated $CaHPO_4$ powders.

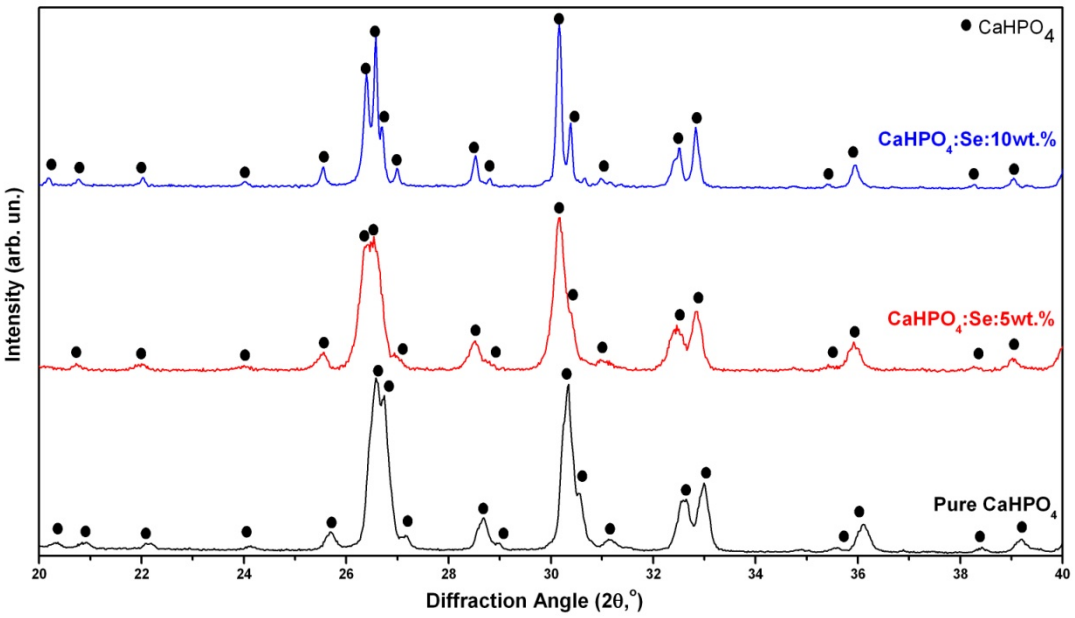

Figure 4.1 The XRD diffractogram of the synthesized pure $CaHPO_4$, $CaHPO_4$:Se:5wt.% and $CaHPO_4$:Se:10wt.% (all peaks correspond to $CaHPO_4$ with JCPDS 09-080)

As it can be seen from Figure 4.1 all peaks of XRD diffractogram shows that phase pure $CaHPO_4$ was obtained for all pure $CaHPO_4$, $CaHPO_4$:Se:5wt.% and $CaHPO_4$:Se:10wt.%. Neither the other intermediate phases of calcium phosphates nor Se-compounds were formed in the structure.

The SEM micrographs of pure $CaHPO_4$, $CaHPO_4$:Se:5wt.% and $CaHPO_4$:Se:10wt.% are shown in Figure 4.2. Se-incorporated $CaHPO_4$ crystals have a different microstructure when compared with pure $CaHPO_4$. It can be said that this change is an indirect evidence of Se incorporation. The pure $CaHPO_4$ has a spongy-like microstructure, while Se-containing $CaHPO_4$ crystals exhibit well-defined plate-like forms in reticulated organization.

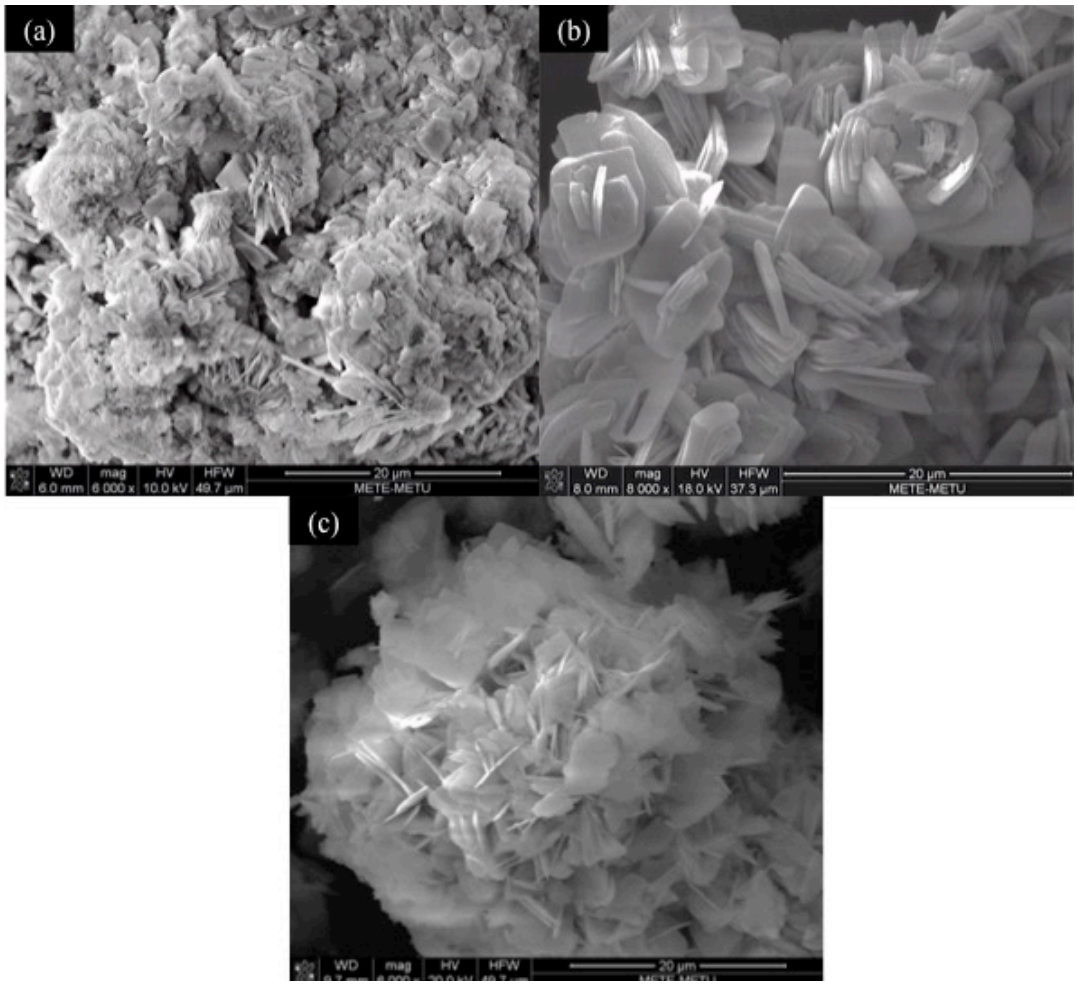

Figure 4.2 SEM micrographs of pure $CaHPO_4$(a), $CaHPO_4$:Se:5wt.%(b) and $CaHPO_4$:Se:10wt.%(c)

$CaHPO_4$ was prepared by precipitating mother solutions of $Ca(OH)_2$ and H_3PO_4 with proper amounts of Se ion-containing Na_2SeO_3 aqueous solution as explained in *Chapter 3*. It was pre-assumed that all Se addition will go into $CaHPO_4$ crystals. However, EDS results shows that there is a limited of Se incorporation as shown by the figures given in Table 4.1. This finding suggests that some of dissolved Se was remained in the main precipitation media (here water-based liquor) and was lost during filtering of the precipitate cake. *From here after, the Se-incorporated (with 5 wt. % or 10 wt. % according to theoretical) systems will be referred in semi-*

quantitative manner as low- and high-Se incorporated product, somewhat overseeing the absolute amount of Se-incorporation

Table 4.1 EDS analysis of pure $CaHPO_4$, $CaHPO_4$:Se:5wt.% and $CaHPO_4$:Se:10wt.% (All EDS results are in wt.%)

Element	$CaHPO_4$	$CaHPO_4$:Se:5wt.%	$CaHPO_4$:Se:10wt.%
Se	0	1.7	4.9
P	38.9	39.2	40.9
Ca	61.1	59.1	54.2

From EDS analyses, it is clearly seen that Se exhibits in $CaHPO_4$ phases with lower amount than the theoretical values. From the XRD results, given in Figure 4.1, the only phase in the structure is $CaHPO_4$. The absence of formation of Se-compounds is a direct evidence of successfully doping Se in $CaHPO_4$ without forming any other phases. Se forms Se–O bonds and replacing for phosphate groups. Figure 4.3 shows the EDS spectrum of pure, 5 wt. % and 10 wt. % Se-incorporated $CaHPO_4$ powders. In order to maintain the charge neutrality destructed by Se ion incorporation, Ca ion content decreases and P ion content increases.

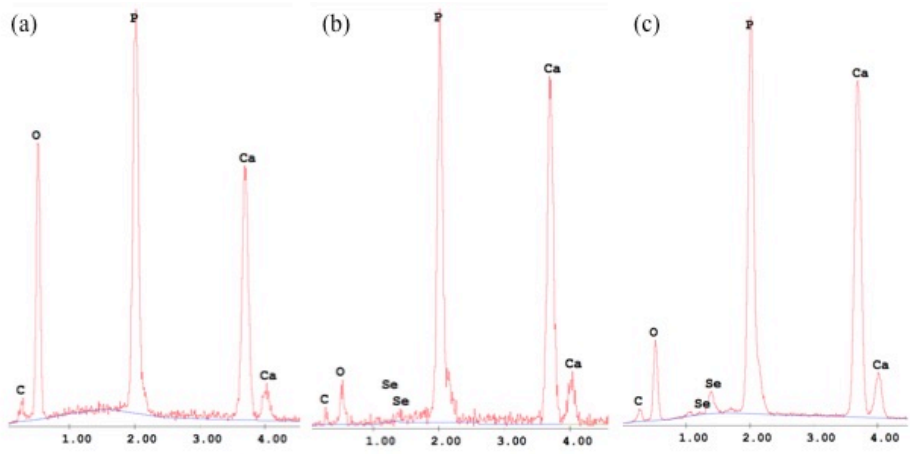

Figure 4.3 EDS spectra of pure $CaHPO_4$(a), $CaHPO_4$:Se:5wt.%(b) and $CaHPO_4$:Se:10wt.%(c)

α-TCP (or α-TCP:Se) was prepared by solid-state reaction of proper amounts $CaCO_3$ and previously synthesized $CaHPO_4$ (or $CaHPO_4$:Se) at 1200 °C, where hot solid mixture mass was air quenched. Figure 4.4 shows the XRD diffractograms of as-synthesized pure α-TCP, α-TCP synthesized using Se-incorporated $CaHPO_4$ particles.

For the pure α-TCP product, all peaks completely match with α-TCP with JDPDS card no 09-348. There is no other diffraction peaks for other calcium phosphate phases, therefore it can be said that phase pure α-TCP is obtained. Because of the effective quenching, β-TCP formation is completely suppressed for all three samples. (Since the only formed polymorph of TCP is α-TCP, it will be referred as TCP only, hereafter.)

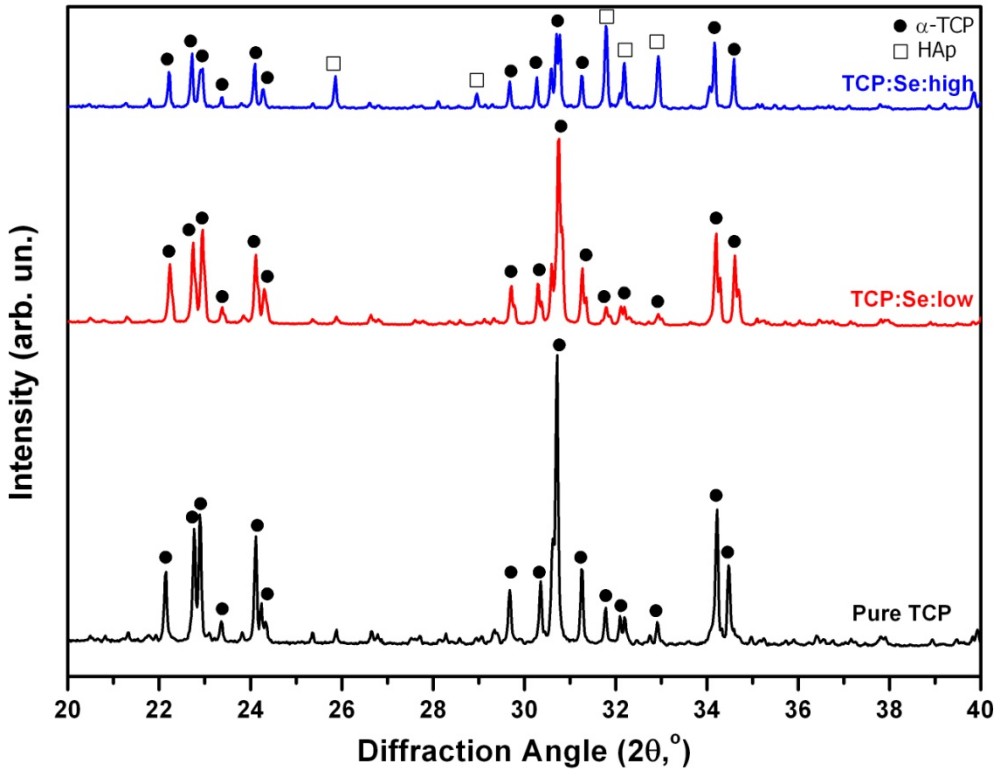

Figure 4.4 The XRD diffractogram of solid-state synthesis products of pure TCP, low-Se-incorporated TCP and high-Se-incorporated TCP (JCPDS 09-348 for α-TCP, JCPDS 09-432 for HAp)

As seen from XRD diffractogram in Figure 4.4, when the amount of Se-incorporation is low the formation of other calcium phosphate compounds is not observed. α-TCP remains phase pure. However, relatively higher amount of Se addition leads the formation of HAp together with α-TCP. This situation may promote cement-type reactivity of α-TCP. Since pre-existing HAp crystals formed in this step may act as nucleation agent/source during hydration of α-TCP to CDHAp ; cement reaction products, i.e. newly formed HAp crystals may grow on the pre-existing HAp crystals.

The SEM micrographs of pure TCP, TCP particles formed using low-Se-incorporated and high-Se-incorporated TCP powders are given in Figure 4.5. All TCP powders exhibit irregularly-shaped granule-like, semi-fused form. This

morphology is characteristic for ceramic powders synthesized by high temperature solid-state reaction as reported previously by Cicek et al. [80]. No morphological variation/change was observed due to use of Se-incorporated $CaHPO_4$ precursor.

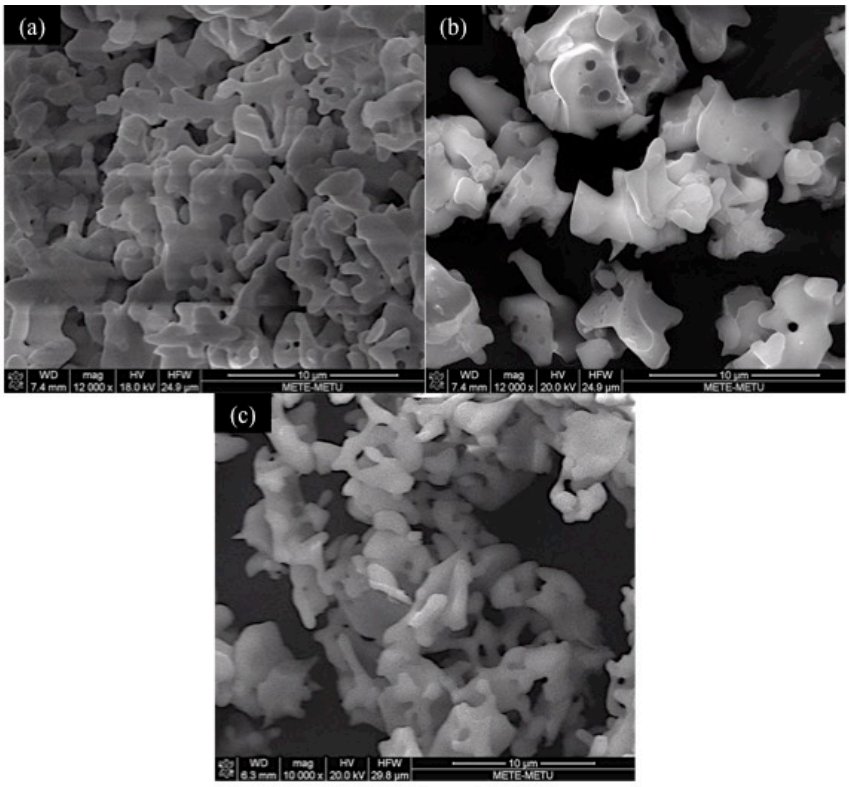

Figure 4.5 SEM micrographs of pure TCP(a), TCP:Se:low(b) and TCP:Se:high(c)

The chemical analyses of pure TCP and TCP particles formed using low- and high-Se-incorporated $CaHPO_4$ powders are represented by the EDS data shown in Table 4.2. As explained before, limited and lower amount Se incorporation was realized in synthesis of $CaHPO_4$. There is an additional lost for Se content when these $CaHPO_4$ powders were employed as a precursor in making TCP powders, as it can be seen by comparing the values in Table 4.1 and Table 4.2. This additional lost of Se may be due to high temperature firing.

Table 4.2 EDS spectra of pure TCP, TCP:Se:low and TCP:Se:high (All EDS results are in wt.%)

Element	TCP	TCP:Se:low	TCP:Se:high
Se	0	1.2	2.2
P	35.9	34.2	31.6
Ca	64.2	64.6	66.2

Further chemical analyses of pure TCP and TCP particles formed using low- and high-Se-incorporated $CaHPO_4$ powders were carried out by FTIR. The transmittance spectra in the range of 2000-400 cm^{-1} are shown in Figure 4.6. The data shows two major bands of phosphate absorption. The bands at around 565 cm^{-1} and 600 cm^{-1} correspond to antisymmetric bending mode of P-O bonds. The bands at 970 cm^{-1}, 1050 cm^{-1} and 1100 cm^{-1} are for symmetric stretching and antisymmetric stretching modes of P-O bonds. No absorption event that can be assigned to Se-O bonding was observed or low- and high-Se-incorporated TCP samples, most likely due to low content of Se addition as revealed by the EDS analyses. (The whole FTIR spectra in the range of 4000-500 cm^{-1} is given in Appendix)

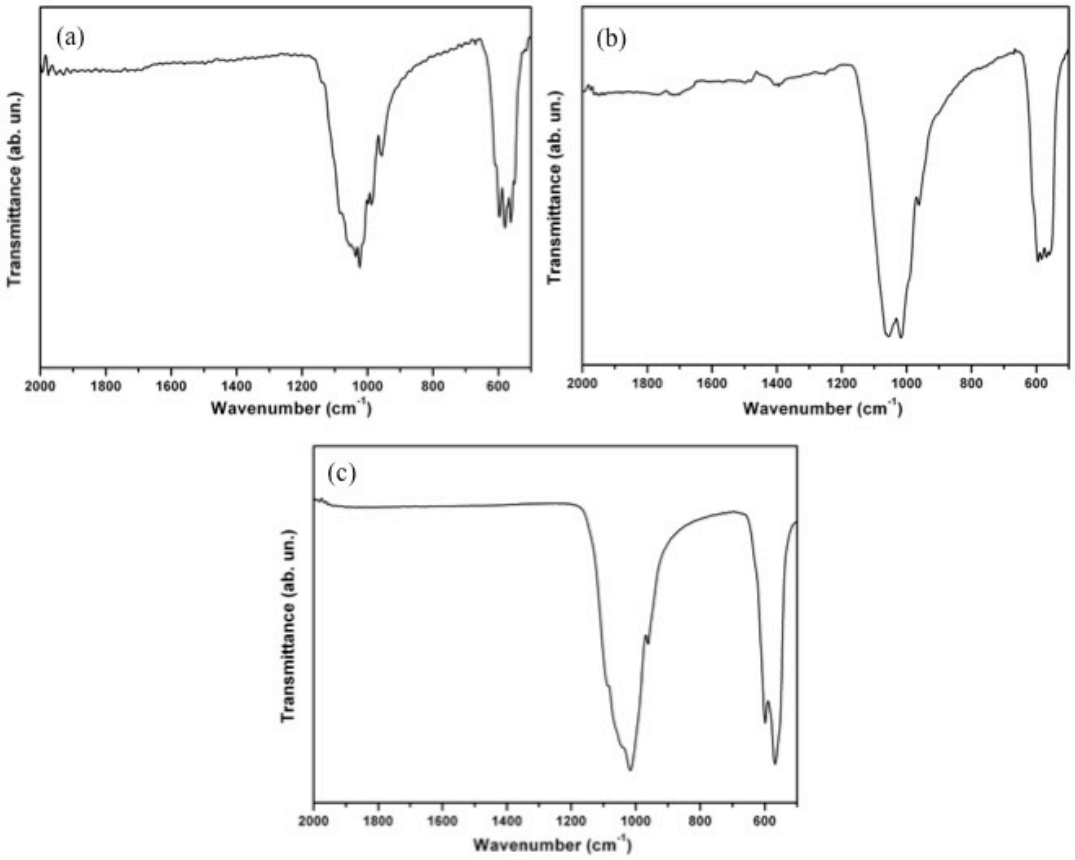

Figure 4.6 FTIR spectra of phosphate regions of pure TCP(a), TCP:Se:low(b) and TCP:Se:high(c) in the range of 2000-500 cm^{-1}

4.2. Cement conversion of TCP samples

4.2.1. Characterization of cement products

After synthesis and characterization of pure, Se-incorporated α-TCP powders, their cement-type reactivity was investigated. All three powders were reacted with DI water at physiological temperature (37 °C) to obtain conversion to hardened end product of CDHAp. Figure 4.7 shows the XRD diffractograms of end products of cement reaction for pure, Se-incorporated α-TCP powders. The data are for resultant products after 48 h of reaction at 37 °C. The reaction was stopped by washing the wet cement end products with acetone and drying them at open atmosphere.

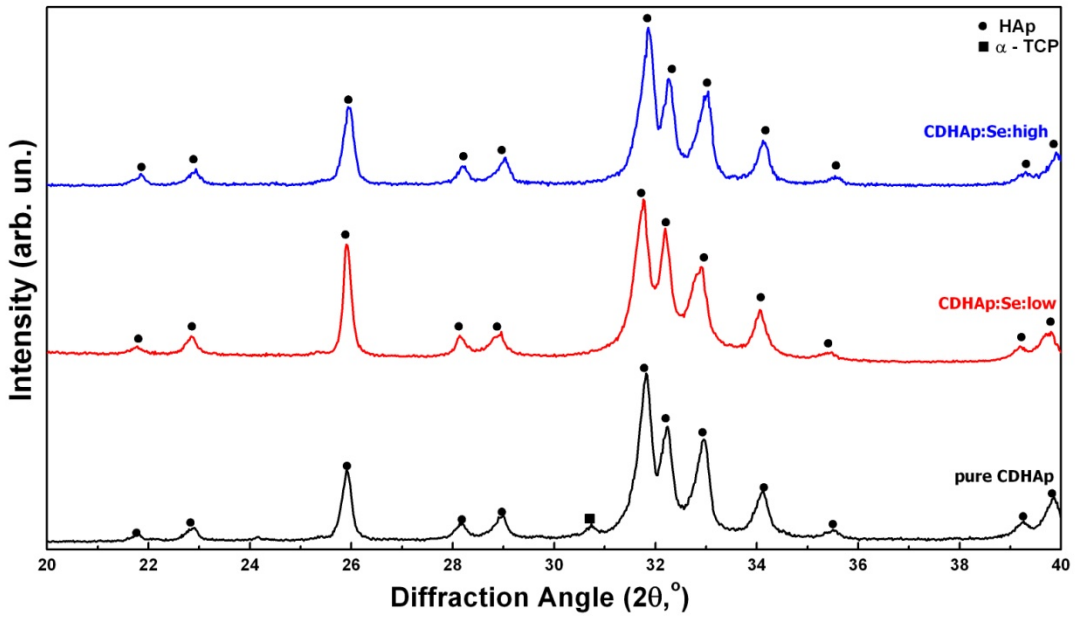

Figure 4.7 XRD diffractograms of hydration products of pure TCP, TCP:Se:low and TCP:Se:high (All peaks correspond to HAp with JCPDS 09-432 and α-TCP with JCPDS 09-348)

XRD diffractograms show that during hydration of pure α-TCP there is a limited transformation to HAp, trace amount of unreacted α-TCP remains for pure reactant; it was not fully converted to HAp. However, Se-incorporated α-TCPs on the other were fully converted to HAp without any remaining reactant phase. This suggests that Se-incorporation enhances hydraulic reactivity and cement reaction kinetics.

SEM micrographs given in Figure 4.8 show the microstructure of end product of CDHAp particles and gives information about hardening by hydration of α-TCP powders. All CDHAp crystals exhibit reticulated needle/plate like morphology which are similar with the results reported previously [81]. This morphology change from granular shaped ceramics to flake-like morphology is typical for the self-setting reactions of dissolution and precipitation and characteristic to cement-type hydration leading to hardening. The morphologies of CDHAp cement products have no distinct change with Se-incorporation as seen from comparing Figure 4.8(a) with Figure 4.8(b) and Figure 4.8(c).

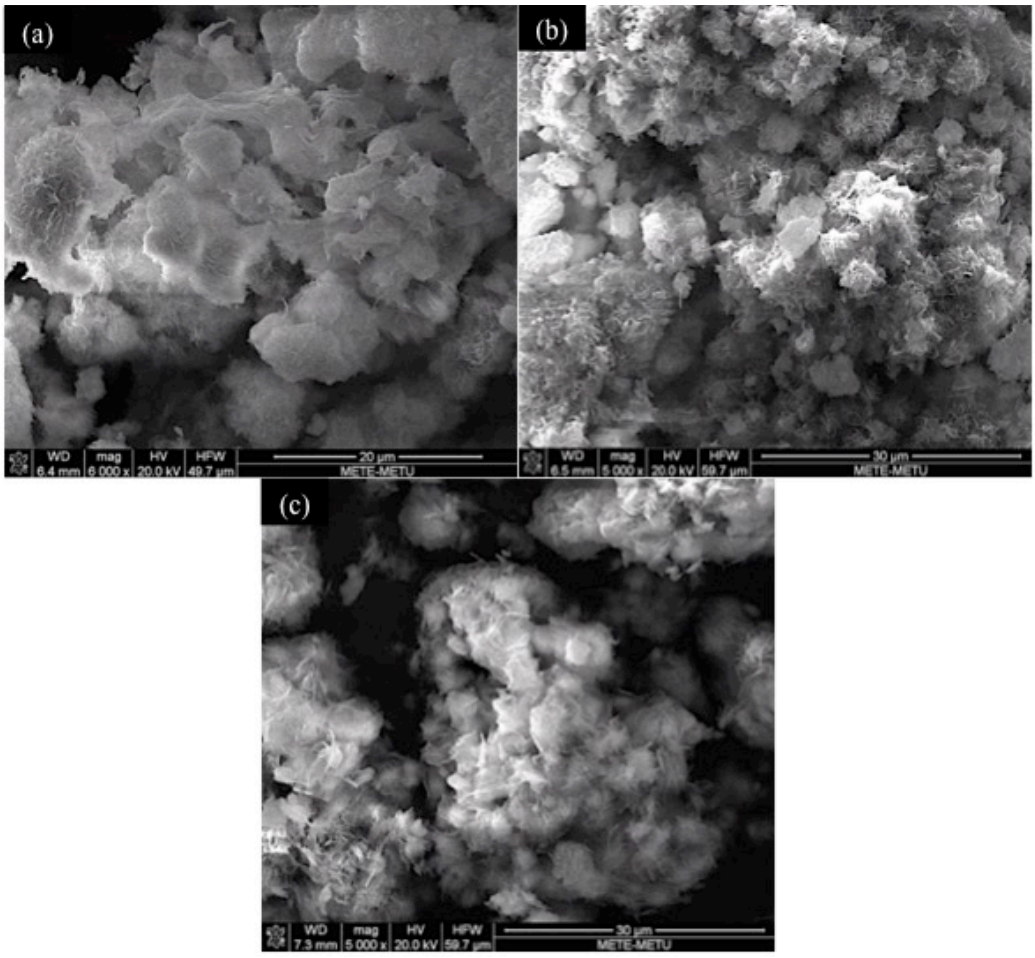

Figure 4.8 SEM micrograph of hydration product of pure α-TCP(a), α-TCP:Se:low(b) and α-TCP:Se:high(c)

The EDS spectra results of hydration products of pure TCP and TCP particles formed using low- and high-Se-incorporated $CaHPO_4$ powders, which are referred as pure CDHAp, low-Se-incorporated and high-Se-incorporated CDHAp, respectively, are given in Table 4.3. Se amounts in CDHAp cements are again lower than the aimed/theoretical values, as in $CaHPO_4$ and α-TCP powders. The detection limitations and related errors of EDS can be related with this difference of the amounts. Moreover, Se addition does not fully incorporate to the CDHAp structure, there are some lost of Se during precipitating $CaHPO_4$. In addition, during firing

some amount of Se was again lost. However, it is seen that hydration reaction with water does no effect the final amount of Se in the structure.

Table 4.3 EDS spectra of hydrated cement products which are pure CDHAp, CDHAp:Se:low and CDHAp:Se:high (All EDS results are in wt.%)

Element	CDHAp	CDHAp:Se:low	CDHAp:Se:high
Se	0	1.4	3.1
P	32.6	34.1	33.3
Ca	67.4	64.5	63.6

In order to reveal the chemical structure of hydration products-that are partially or fully converted to HAp based on in XRD results- FTIR analyses were performed. XRD and SEM results are insufficient for understanding the chemical nature of HAp, the stoichiometry (Ca/P ratio) and presence of chemical groups can not be understood from XRD results. For example, stoichiometric HAp with Ca/P ratio of 1.67 and calcium-deficient HAp with Ca/P ratio of 1.5 are identical in XRD analysis, however the presence of $(HPO_4)^{2-}$ and OH^- in CDHAp can be easily seen by FTIR spectroscopy.

Figure 4.9 shows the FTIR spectra of hydrated cement products of pure, low- and high-Se-incorporated α-TCP. There are some differences between the hydrated products and unhydrated ones which are given in Figure 4.6. The bands at around 565 cm^{-1} and 600 cm^{-1} for antisymmetric bending mode of P-O bonds are distinctly seperated after hydrating the TCP powders. There is a change in the other phosphate group absorption band at 970 cm^{-1}, 1050 cm^{-1} and 1100 cm^{-1}. The phosphate groups are common in both TCP and hydrated products, however, the differences are because of the change in crystal structure and bonding variations. The additional two peaks at around 860-870 cm^{-1} and 620-630 cm^{-1} are for $(OH)^-$ librational mode and

P-OH streching of $(HPO_4)^{2-}$, respectively [81]. The formation of $(HPO_4)^{2-}$ proves the formation of calcium-deficient HAp (CDHAp).

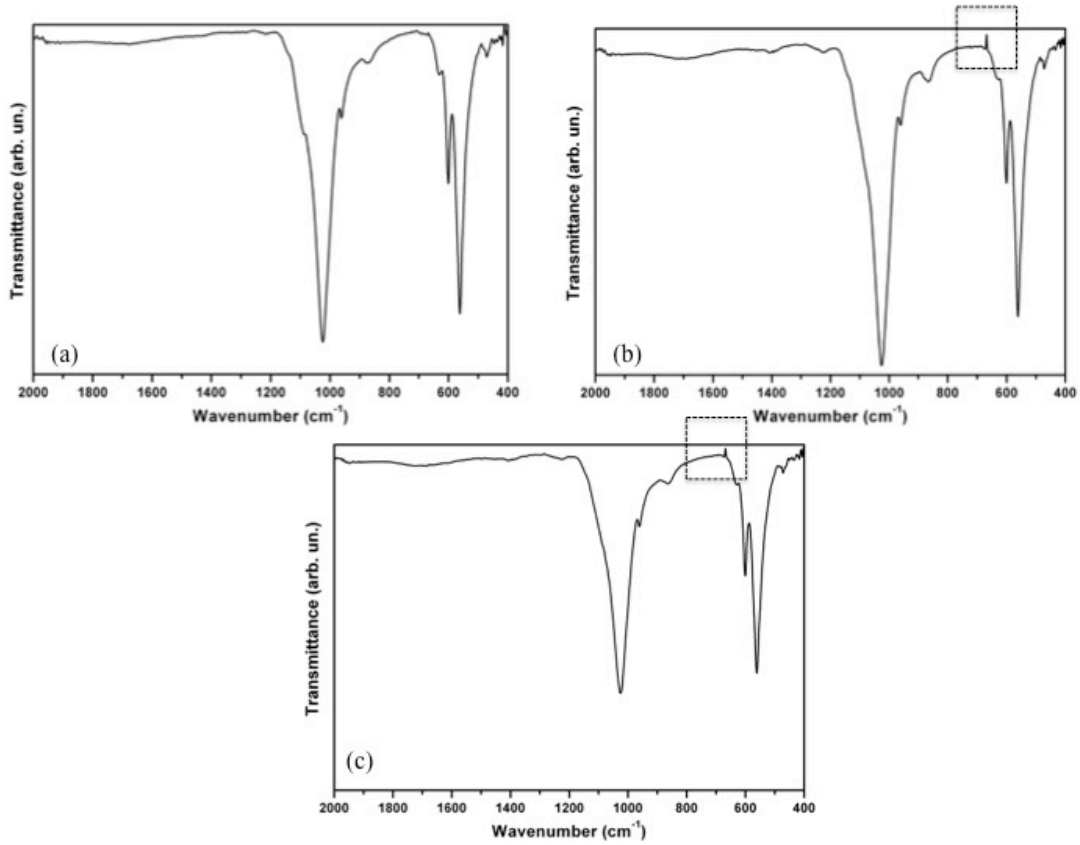

Figure 4.9 FTIR spectra of hydration products of pure TCP(a), TCP:Se:low(b) and TCP:Se:high(c) in the range of 2000-400 cm^{-1}

Furthermore, the regions shown in dashed boxes are the additional peaks for Se incorporated samples showing weak absorption signals. The bands at around 668 cm^{-1} are attributed to vibration of Se-O of H_2SeO_3 [82]. Because of the low content of Se incorporation, which is given in EDS spectra results in Table 4.3, the Se-O absorption peaks are weak in the FTIR spectra. The formation of additional peaks for Se-O bonds is the direct evidence of incorporation of Se ions in the hydrated cement

product. (The whole FTIR spectra in the range of 4000-450 cm^{-1} is given in Appendix)

4.2.2. Study of hydration kinetics of TCP samples

After investigating the physical/chemical characteristics of hydrated products of α-TCP samples, further analysis were done to evaluate its cement-type reaction kinetics. XRD results give information about the phases present in the structure. However, it is limited in revealing details conversion kinetics. In order to examine the hydrolysis kinetics, it is important to determine when exactly the reaction starts. Any aqueous reaction involves heat absorption or heat evolution, i.e. endothermic or exothermic reactions. The rate of heat release or adsorption can be monitored during the reaction at a constant temperature and this is related with the reaction kinetics. For this purpose isothermal calorimetry is used to elucidate the cement type reactivity of pure, Se-incorporated α-TCP powders. Comparison of the hydration kinetics of these three powders was done by using isothermal calorimetry. Figure 4.10, Figure 4.11 and Figure 4.12 shows isothermal calorimetry data (dQ/dt versus time) of hydration of pure α-TCP, low-Se-incorporated α-TCP and high-Se-incorporated α-TCP, respectively. The reaction temperature for all samples is 37 °C. These curves show the heat evolution during reaction between α-TCP and DI water. For all three samples, the solid to liquid ratio is constant, 1:2.

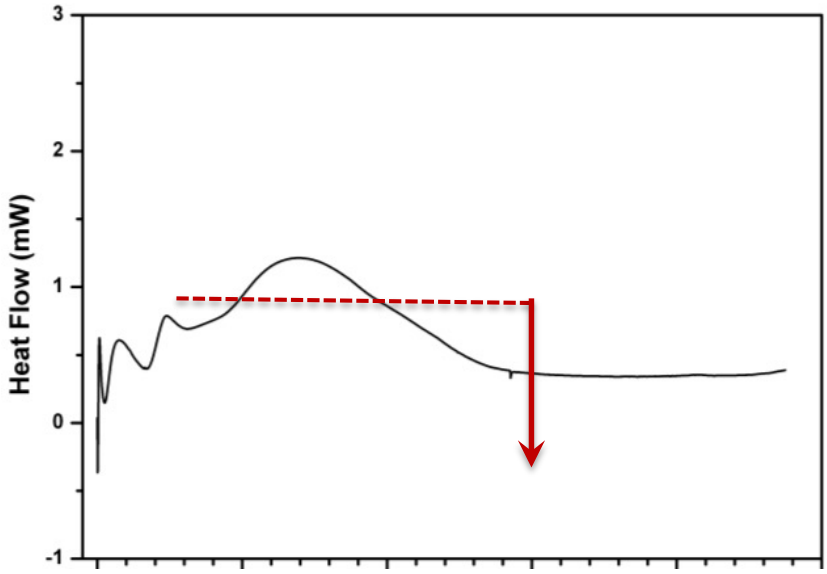

Figure 4.10 dQ/dt vs. time data for chemical reaction between pure α-TCP and DI water

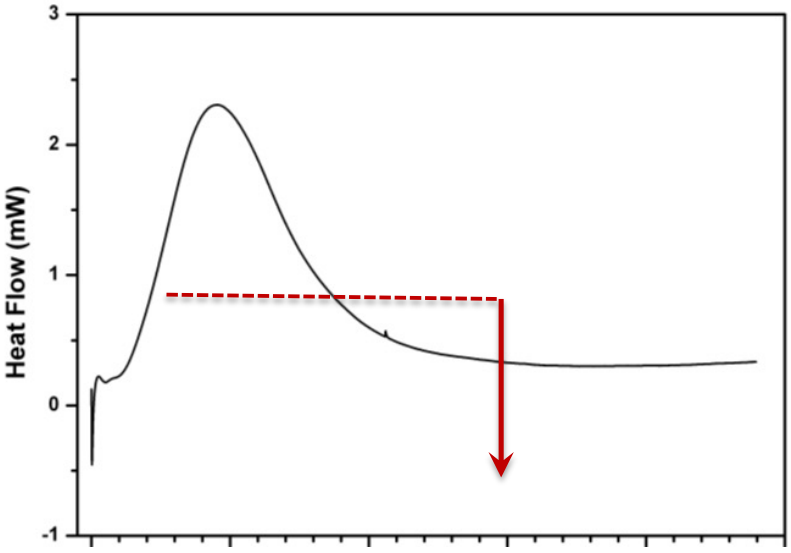

Figure 4.11 dQ/dt vs. time data for chemical reaction between α-TCP:Se:low and DI water

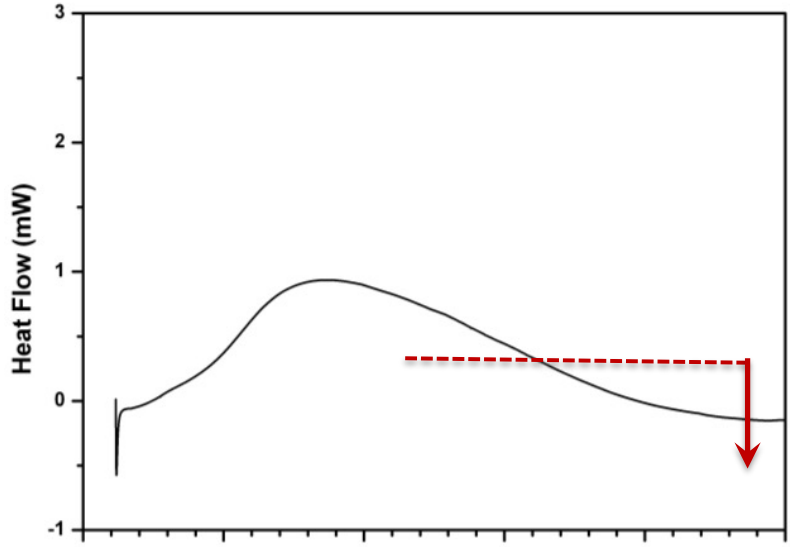

Figure 4.12 dQ/dt vs. time data for chemical reaction between α-TCP:Se:high and DI water

The heat flow curves shown in Figure 4.10, Figure 4.11 and Figure 4.12 indicate that the hydration reaction of α-TCP samples was exothermic reaction. The completion of conversion was understood when the heat flow becomes steady at around zero. It is seen from heat flow curves that Se-incorporation changes the reaction kinetics and mechanistic path from α-TCP to CDHAp cement conversion. The heat events are related with the nucleation and growth of new phases. As seen from Figure 4.10 that there are two sharp peaks at around 1h and 5h and one more broad peak spreading out longer times. The first sharp peak can be related with wetting the α-TCP powders then the other sharp peak corresponds to nucleation of new phases. The broad peak can represent the growth of newly formed phases. However, the mechanism is different for Se-incorporated α-TCP powders' heat flow curves, given in Figure 4.11 and Figure 4.12. For low-Se-incorporated α-TCP powder, there are one short sharp peak and one broad main peak in its heat flow curve, given in Figure 4.11. It can be said that wetting of α-TCP powders and nucleation of new phase

occurs in short time with one heat-involving event. This situation is different for high-Se-incorporated α-TCP powder's heat flow curve, given in Figure 4.12. Overall setting occurs by a single broad heat-involving event with only a main peak. This can be explained by the XRD result of α-TCP:Se:high powder given in Figure 4.4. While obtaining α-TCP by solid-state reaction from inorganic precursors, small amount of HAp was formed in the structure together with α-TCP. The previously formed HAp may act as nucleation agent for the hydration kinetics, which means that newly formed CDHAp crystals may be nucleated on the pre-form HAp crystals. Therefore, this may be the reason of not observing the nucleation heat event peak during hydration of powders.

The total time of the reaction and total heat outcome are calculated by integrating dQ/dt vs. time curves of the reaction of pure α-TCP, low- and high-Se-incorporated α-TCP with DI water, given in Figure 4.13. The calculated values are given in Table 4.4 for all samples.

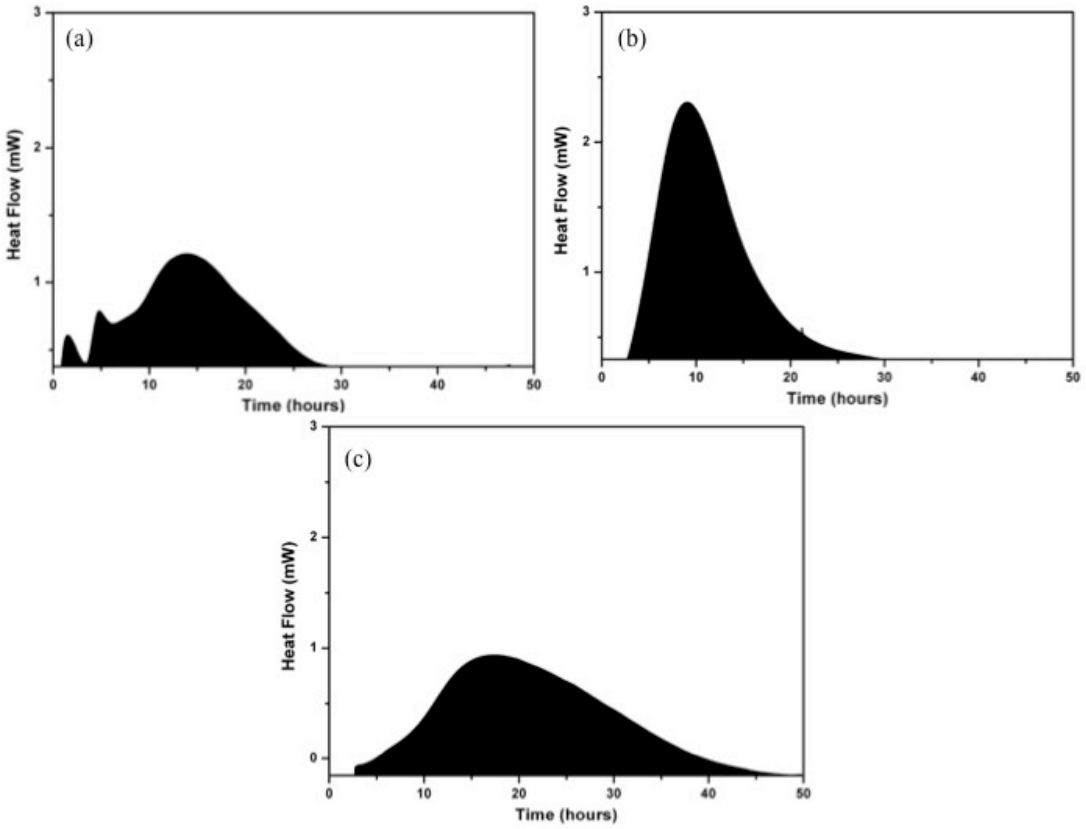

Figure 4.13 Integrated dQ/dt vs. time curves for pure CDHAp(a), CDHAp:Se:low(b) and CDHAp:Se:high(c) cements

Table 4.4 Approximate total reaction time and total heat outcome values obtained from integrated dQ/dt vs. time graphs of pure CDHAp, CDHAp:Se:low and CDHAp:Se:high cements

	Approximate total reaction time	**Total heat outcome**
Pure CDHAp	30 h	72 ± 5 J/g
CDHAp:Se:low	30 h	84 ± 5 J/g
CDHAp:Se:high	48 h	86 ± 5 J/g

The total heat outcome of the reactions between pure, low- and high-Se-incorporated α-TCP and DI water are given in Table 4.4. The total heat outcome values of Se-incorporated powders are higher than the pure sample. This can be explained by the

phases present in the structure after the reaction. As it is seen in Figure 4.7b and Figure 4.7c, Se-incorporated α-TCP powders are fully converted to CDHAp when reacted with DI water. There is no unreacted reactant, i.e. no α-TCP was remained in the system. However, this is not valid for pure α-TCP powder. After reacting pure α-TCP with DI water, as seen from Figure 4.7a, trace amount of unreacted α-TCP is left in the system. The fully conversion from α-TCP to CDHAp of Se-incorporated α-TCPs results in higher heat outcome.

The total reaction time was determined by the fact that heat flow becomes stable at around zero. When the reaction time of three samples is compared, it is seen that conversion from high-Se-incorporated α-TCP to CDHAp requires more time than the other two samples. The completion of reaction of pure α-TCP to CDHAp and low- Se-incorporated α-TCP to CDHAp is about 30 h, while this time for high-Se-incorporated α-TCP to CDHAp is about 48 h. Higher amount of Se addition slows down the cement-type conversion reaction. Although the complete conversion from α-TCP to CDHAp times are different for low- and high-Se-incorporated α-TCP powders, heat flow versus time curves are similar. There is no low intensity short peak corresponding to nucleation of new phase, but there is a broad high intensity peak stabiling at zero for completing the conversion for both samples. However, the intensity of this broad peak is different for these two samples. For low-Se-incorporated CDHAp, broad peak has higher intensity, while this peak for high-Se-incorporated CDHAp has lower intensity but broader than the former one. This intensity difference can be explained by the total heat outcome values and total time for the reaction. The total conversion time for low-Se-incorporated CDHAp cement is 30 h, this time for high-Se-incorporated CDHAp cement is 48 h. In order to complete the conversion with similar heat outcome values, the intensity of the broad peak is expected to be different for these two cement systems.

Since higher amount of Se addition slows down the cement-type conversion, lower Se-incorporation is ideal in terms of both cement-type conversion reaction time and

obtaining fully CDHAp as a final product without any reactant left in the structure. Figure 4.14 shows the XRD results of hydration product of low-Se-incorporated α-TCP with 2h, 4h, 8h, 12h, 24h and 48h of reaction.

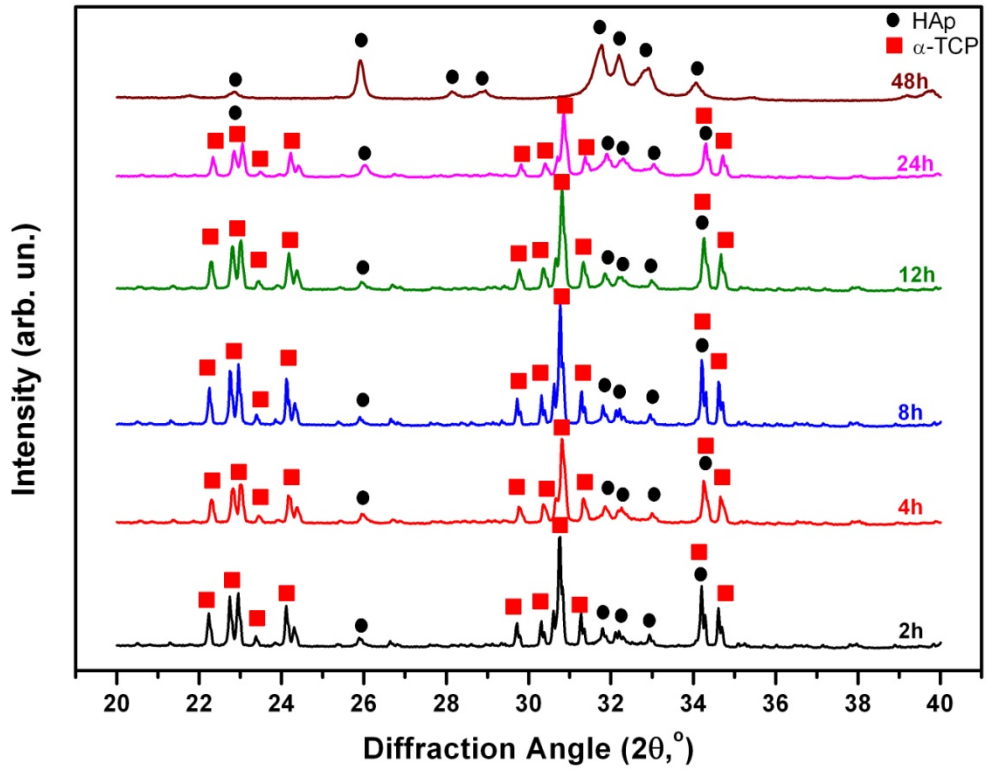

Figure 4.14 XRD diffrctogram of hydrated product of α-TCP:Se:low with different times of reaction (All peaks correspond to HAp with JCPDS 09-432 and α-TCP with JCPDS 09-348)

The phase change of lower Se-incorporated α-TCP reacting with DI water for cement-type conversion with different times of reaction is given in Figure 4.14. At 48 h of reaction all α-TCP fully converted to HAp without any reactant left in the system. However, at 2 h of reaction, the amount of newly formed HAp crystals is very low, as expected. From 2 h to 48 h of reaction α-TCP amount decreases and HAp amount increases in the structure. At 24 h of reaction, the intensity of HAp

peaks is higher than 2 h, 4 h, 8 h and 12 h. However, fully conversion is not observed at 24 h of reaction. This is an expected result, since the total reaction time was obtained approximately 30 h, as shown in Table 4.4. The most intense peak of α-TCP is at around 31°, while the most intense peak of HAp is at around 32°. As it is seen from Figure 4.14, as time of reaction increases, the most intense peak of α-TCP decreases, the most intense peak of HAp increases. From these findings, it is seen that with increasing the time of reaction, α-TCP was consumed in producing HAp.

CHAPTER 5

CONCLUSIONS

α-TCP, Se-incorporated α-TCP were synthesized by solid-state reaction of required amounts of inorganic precursors. Effect of different amounts of Se-incorporation on the structure of α-TCP was investigated using complementary characterization techniques. Moreover, the cement-type reactivity from α-TCP to hardened end product CDHAp of these synthesized powders were examined. The effect of Se on the hydration kinetics was investigated in detail. The general results of this thesis are given as follows.

Synthesis and characterization of α-TCP and Se-incorporated α-TCP powders: Phase pure α-TCP was synthesized by solid-state reaction between previously synthesized $CaHPO_4$ and $CaCO_3$. For synthesis of Se-incorporated α-TCP (α-TCP:Se with aimed concentrations of 5wt. % and 10wt. %) Se incorporated into $CaHPO_4$ during aqueous precipitation of this TCP precursor. $CaHPO_4$:Se powders were similarly reacted with $CaCO_3$ to obtain α-TCP:Se. Se incorporation in $CaHPO_4$ did not lead to formation of other calcium phosphate phase(s) or Se compound(s). However, for α-TCP powders, high amount of Se addition leads to formation of HAp in addition to α-TCP crystals. The chemical analyses showed that Se-incorporation occurred in a limited extent lower than theoretical/aimed values. After high temperature solid-state reaction between Se-incorporated $CaHPO_4$ and $CaCO_3$, additional lost of Se amount was observed. No morphological change was found for α-TCP powders due to Se addition. All pure and Se-incorporated α-TCPs show semi-fused particulate morphology characteristic to ceramics obtained by high temperature solid-state reactions.

Cement-type reactivity and cement characteristics of α-TCP and Se-incorporated α-TCP powders: Pure and Se-incorporated α-TCP powders were converted into CDHAp cement by mixing with DI water with liquid to solid ratio of 2:1 at physiological temperature, i.e. 37 °C. The microstructural and morphological properties of hydration product of CDHAp cement remain unaffected by Se addition; pure CDHAp and Se-incorporated CDHAps exhibited the same plate-like microstructure. Hydration product of pure α-TCP was not fully converted to CDHAp and trace amount of α-TCP was remained in the end product. However, Se-incorporated α-TCPs fully converted to CDHAp without any reactant remain. High extent of Se addition led to formation of HAp besides α-TCP in synthesis. In this case, pre-existing HAp acted as nucleation agent for HAp crystals formed by cement conversion. The FTIR analyses proved calcium deficiency and stoichiometry of hardened cement product. It was shown that complete cement-type conversion from α-TCP to CDHAp still occurred by Se modification. However, overall setting (cement conversion) occurred by a different mechanistic way by Se addition. The conversion of pure α-TCP to CDHAp cement occurred by two short intense peaks, which are wetting and nucleation of new phase, and one broad peak, which is growth of newly nucleated phase. However, this conversion from Se-incorporated α-TCPs to CDHAps occurred with a single heat event. This difference may show a synergetic/positive effect of Se addition. However, the total reaction times are different. Higher amount of Se addition slows down the cement-type conversion. Therefore, the optimum amount of Se favoring hydration kinetics in obtaining phase pure reactants and products seem to less than 2 wt. %.

REFERENCES

[1] Park, J. and Lakes, R. S. *Biomaterials: An introduction: Third edition*. (2007).

[2] Weiner, S. and Wagner, H. D. "The Material Bone: Structure-Mechanical Function Relations," *Annu. Rev. Mater. Sci.*, 28, 271–298 (1998).

[3] Reznikov, N., Shahar, R. and Weiner, S. "Bone hierarchical structure in three dimensions," *Acta Biomater.*, 10, 3815–3826 (2014).

[4] Wang, Y. et al. "The predominant role of collagen in the nucleation, growth, structure and orientation of bone apatite," *Nat. Mater.*, 37, 112–116 (2012).

[5] Rho, J., Kuhn-Spearing L. and Zioupos P., "Mechanical properties and the hierarchical structure of bone Jae-Young," *Med. Eng. Phys.*, 92, 92–102 (1998).

[6] Kuhn-Spearing L, G. M., Rey C., Kim, H.M. "Carbonated apatite nanocrystals of bone. Synthesis and processing of nanocrystalline powder," *Miner. Met. Mater. Soc.* (1996).

[7] Yusufoğlu, Y. "Synthesis and characterization of carbonated hydroxyapatite and bioinspired polymer-calcium phosphate nanocomposites.," (2009).

[8] Burger, C. *et al.*, "Lateral Packing of Mineral Crystals in Bone Collagen Fibrils," *Biophys. J.*, 95, 1985–1992 (2008).

[9] Dorozhkin, S. V. "Biocomposites and hybrid biomaterials based on calcium orthophosphates," 2535 (2011).

[10] Wilson, E. E., Awonusi, A., Morris, M. D., Kohn, D. H., Tecklenburg, M. M. J. and Beck, L. W. "Three structural roles for water in bone observed by solid-state NMR," *Biophys. J.*, 90, 3722–3731 (2006).

[11] Lieberman, J. R. and Friedlaender, G. E. *Bone regeneration and repair: biology and clinical applications.* Humana Press (2005).

[12] Vaccaro, A. R. *et al.*, "Bone grafting alternatives in spinal surgery," *Spine J.*, 2, 206–215 (2002).

[13] Moore, W. R., Graves, S. E. and Bain, G. I. "Synthetic Bone Graft Substitutes," 354–361 (2001).

[14] Albrektsson T. and Johansson C. "Osteoinduction, osteoconduction and osseointegration," *Eur. Spine J.*, 10, S96–S101 (2001).

[15] Kelly, C. M., Wilkins, R. M., Gitelis, S., Hartjen, C., Watson, J. T. and Kim, P. T. "The Use of a Surgical Grade Calcium Sulfate as a Bone Graft Substitute," *Clin. Orthop. Relat. Res.*, 382, 42–50 (2001).

[16] Singh, N. B. and Middendorf, B. "Calcium sulphate hemihydrate hydration leading to gypsum crystallization," *Prog. Cryst. Growth Charact. Mater.*, 53, 57–77 (2007).

[17] Hu, G., Xiao, L., Fu, H., Bi, D., Ma, H. and Tong, P. "Study on injectable and degradable cement of calcium sulphate and calcium phosphate for bone repair," *J. Mater. Sci. Mater. Med.*, 21, 627–634 (2010).

[18] Dorozhkin, S. V. "Calcium Orthophosphates as Bioceramics: State of the Art," *J. Funct. Biometer.*, 1, 22–107 (2010).

[19] Albee F. H. and Morrison, H. F. "Studies in Bone Growth: triple calcium phosphate as a stimulus osteogenesis," *Ann. Surg.*, 71, 32–39 (1920).

[20] Ray, R., Degge, J., Gloyd, P. and Mooney, G. “Bone regeneration,” *J. Bone Jt. Surg.*, 638–647 (1952).

[21] Bohner, M. “Calcium orthophosphates in medicine: From ceramics to calcium phosphate cements,” *Injury*, (2000).

[22] Dorozhkin, S. V. “Self-Setting Calcium Orthophosphate Formulations,” *J. Funct. Biomater.*, 4, 209–311 (2013).

[23] Dorozhkin, S. V. “Bioceramics of calcium orthophosphates,” *Biomaterials*, 31, 1465–1485 (2010).

[24] Jarcho, M., Bolen, C. H., Thomas, M. B., Bobick, J., Kay, J. F. and Doremus, R. H. “Hydroxylapatite synthesis and characterization in dense polycrystalline form,” *J Mater Sci*, 11, 2027–2035 (1976).

[25] De Groot, K. “Bioceramics consisting of calicum phosphate salts,” *Biomaterials*, 1, 47–50 (1980).

[26] Akao, M, Aoki, H. and Kato, K. “Mechanical properties of sintered hydroxyapatite for prosthetic applications,” *J. Mater. Sci. Mater. Med.*, 16, 809–812 (1981).

[27] Kukubo, T. Bioceramics and their clinical applications. Elsevier (2008).

[28] Kohn, M., Rakovan, J. and Hughes, J. M. *Phosphates: geochemical, geobiological and materials importance*. Mineral Society of America, Washington, DC (2002).

[29] Dorozhkin, S. V. “Calcium orthophosphates,” *J. Mater. Sci.*, 42, 1061–1095 (2007).

[30] Dorozhkin, S. V. “Nanodimensional and nanocrystalline apatites and other calcium orthophosphates in biomedical engineering, biology and medicine,” *Materials (Basel).*, 2, 1975–2045 (2009).

[31] Dorozhkin, S. V. “Calcium orthophosphates in nature, biology and medicine,” *Materials (Basel).*, 2, 399–498 (2009).

[32] Carrodeguas, R. G. and De Aza, S. “α-Tricalcium phosphate: Synthesis, properties and biomedical applications,” *Acta Biomater.*, 7, 3536–3546 (2011).

[33] Nikaido, T. *et al.*, “Fabrication of β-TCP foam: Effects of magnesium oxide as phase stabilizer on its properties,” *Ceram. Int.*, 41, 14245–14250 (2015).

[34] Ogose, A. *et al.*, “Histological examination of β-tricalcium phosphate graft in human femur,” *J. Biomed. Mater. Res.*, 63, 601–604 (2002).

[35] Camiré, C. L., Saint-Jean, S. J., Hansen, S., McCarthy, I. and Lidgren, L. “Hydration characteristics of α-tricalcium phosphates: Comparison of preparation routes,” *J. Appl. Biomater. Biomech.*, 3, 106–111 (2005).

[36] Bohner, M., Brunner, T. J., Doebelin, N., Tang, R. and Stark, W. J. “Effect of thermal treatments on the reactivity of nanosized tricalcium phosphate powders,” *J. Mater. Chem.*, 18, 4460–4467 (2008).

[37] Kitamura, M., Ohtsuki, C., Iwasaki, H., Ogata, S. I., Tanihara, M. and Miyazaki, T. “The controlled resorption of porous α-tricalcium phosphate using a hydroxypropylcellulose coating,” *J. Mater. Sci. Mater. Med.*, 15, 1153–1158 (2004).

[38] Khairoun, I., Boltong, M. G., Driessens, F. C. M. and Planell, J. A. “Limited compliance of some apatitic calcium phosphate bone cements with clinical requirements,” *J. Mater. Sci. Mater. Med.*, 9, 667–671 (1998).

[39] Khairoun, I., Boltong, M. G., Driessens, F. C. M. and Planell, J. A. "Some factors controlling the injectability of calcium phosphate bone cements," *J. Mater. Sci. Mater. Med.*, 9, 425–428 (1998).

[40] Dalby, M. J., Di Silvio, L., Harper, E. J. and Bonfield, W. "Increasing hydroxyapatite incorporation into poly(methylmethacrylate) cement increases osteoblast adhesion and response," *Biomaterials*, 23, 569–576 (2002).

[41] Lu, J. X. *et al.*, "Human biological reactions at the interface between bone tissue and polymethylmethacrylate cement," *J. Mater. Sci. Mater. Med.*, 13, 803–809 (2002).

[42] Vazquez, B. *et al.*, "Application of tertiary amines with reduced toxicity to the curing process of acrylic bone cements," *J. Biomed. Mater. Res.*, 34, 129–136 (1997).

[43] Kim, S. B. *et al.*, "The characteristics of a hydroxyapatite-chitosan-PMMA bone cement," *Biomaterials*, 25, 5715–5723 (2004).

[44] LeGeros, R. Z. "Apatite calcium phosphate: possible restrative materials," *J. Dent Res.*, 61 (1982).

[45] Brown, W. E. and Chow, L. "A new calcium phosphate water setting cement," *Cem. Res. Prog.*, 352–379 (1986).

[46] Lemaitre, J., Mirtchi, A. and Mortier, A. "Calcium phosphate cements for medical use: state of the art and perspectives of development," *Silic. Ind.*, 52, 141–146, (1987).

[47] Dorozhkin, S. V. "Calcium orthophosphate cements and concretes," *Materials (Basel).*, 2, 221–291 (2009).

[48] Bohner, M., Van Landuyt, P., Merkle, H. P. and Lemaitre, J. "Composition effects on the pH of a hydraulic calcium phosphate cement," *J. Mater. Sci.*

Mater. Med., 8, 675–681 (1997).

[49] Constantz, B. R. *et al.*, "Histological, chemical, and crystallographic analysis of four calcium phosphate cements in different rabbit osseous sites," *J. Biomed. Mater. Res.*, 43, 451–461 (1998).

[50] Ikenaga, M., Hardouin, P., Lemaître, J., Andrianjatovo, H. and Flautre, B. "Biomechanical characterization of a biodegradable calcium phosphate hydraulic cement: A comparison with porous biphasic calcium phosphate ceramics," *J. Biomed. Mater. Res.*, 40, 139–144 (1998).

[51] Ishikawa, K., Takagi, S., Chow, L. C. and Ishikawa, Y. "Properties and mechanisms of fast-setting calcium phosphate cements," *J. Mater. Sci. Mater. Med.*, 6, 528–533 (1995).

[52] Monma H. and Kanazawa, T. "The hydration of a-tricalcium phosphate," *J Ceram Sec Jpn*, 84, 209–213 (1976).

[53] Bohner, M. "Reactivity of calcium phosphate cements," *J. Mater. Chem.*, 17, 3980–3986 (2007).

[54] Bohner, M., Malsy, A. K., Camiré, C. L. and Gbureck, U. "Combining particle size distribution and isothermal calorimetry data to determine the reaction kinetics of α-tricalcium phosphate-water mixtures," *Acta Biomater.*, 2, 343–348 (2006).

[55] Durucan, C. and Brown, P. W. "Reactivity of α-tricalcium phosphate," *J. Mater. Sci.*, 37, 963–969 (2002).

[56] Dorozhkin, S. V. "Calcium orthophosphate cements for biomedical application,", 3028–3057 (2008).

[57] Bose, S., Tarafder, S., Edgington, J. and Bandyopadhyay, A. "Calcium phosphate ceramics in drug delivery," *Jom*, 63, 93–98 (2011).

[58] Takechi, M. *et al.*, "Effects of added antibiotics on the basic properties of anti-washout- type fast-setting calcium phosphate cement," *J. Biomed. Mater. Res.*, 39, 308–316 (1998).

[59] Ratier, I. G., Best, S. M., Freche, M., Lacout, J. L. and Rodriguez, F. "Behaviour of a calcium phosphate bone cement containing tetracycline hydrochloride or tetracycline complexed with calcium ions," *Biomaterials*, 22, 897–901 (2001).

[60] Ginebra, M. P., Traykova, T. and Planell, J. A. "Calcium phosphate cements as bone drug delivery systems: A review," *J. Control. Release*, 113, 102–110 (2006).

[61] Ginebra, M. P., Rilliard, A., Fernández, E., Elvira, C., San Román, J. and Planell, J. A. "Mechanical and rheological improvement of a calcium phosphate cement by the addition of a polymeric drug," *J. Biomed. Mater. Res.*, 57, 113–118 (2001).

[62] Otsuka, M., Matsuda, Y., Suwa, Y., Fox, J. L. and Higuchi, W. I. "A novel skeletal drug delivery system using a self-setting calcium phosphate cement. 5: Drug release behavior from a heterogeneous drug-loaded cement containing an anticancer drug," *J. Pharm. Sci.*, 83, 1565–1568 (1994).

[63] Mouriño, V., Cattalini, J. P. and Boccaccini, A. R. "Metallic ions as therapeutic agents in tissue engineering scaffolds: An overview of their biological applications and strategies for new developments," *J. R. Soc. Interface*, 9, 401–419 (2012).

[64] Gielen M. and Tiekink, E. *Metallotherapeutic drugs and metal-based diagnostic agents: the use of metals in medicine*. Wiley&Sons (2005).

[65] Dahl, S. G. *et al.*, "Incorporation and distribution of strontium in bone," *Bone*, 28, 446–453 (2001).

[66] Boanini, E., Gazzano, M. and Bigi, A. "Ionic substitutions in calcium

phosphates synthesized at low temperature," *Acta Biomater.*, 6, 1882–1894 (2010).

[67] Alkhraisat, M. H., Mariño, F. T., Rodríguez, C. R., Jerez, L. B. and Cabarcos, E. L. "Combined effect of strontium and pyrophosphate on the properties of brushite cements," *Acta Biomater.*, 4, 664–670 (2008).

[68] Jegou Saint-Jean, S., Camiré, C. L., Nevsten, P., Hansen, S. and Ginebra, M. P. "Study of the reactivity and in vitro bioactivity of Sr-substituted α-TCP cements," *J. Mater. Sci. Mater. Med.*, 16, 993–1001 (2005).

[69] Price, C. T., Koval, K. J. and Langford, J. R. "Silicon: A review of its potential role in the prevention and treatment of postmenopausal osteoporosisgranite, quartz, and other types of rocks, clays, andgemsinthe Earth'scrust" *Int. J. Endocrinol.* (2013).

[70] Reid, J. W., Tuck, L., Sayer, M., Fargo, K. and Hendry, J. A. "Synthesis and characterization of single-phase silicon-substituted α-tricalcium phosphate," *Biomaterials*, 27, 2916–2925 (2006).

[71] Wei X. and Akinc, M. "Si, Zn-modified tricalcium phosphates: a Phase composition and crystal structure study," *Key Eng. Mater.*, 284–286, 42–49 (2005).

[72] Julien, M. *et al.*, "Physico-chemical-mechanical and in vitro biological properties of calcium phosphate cements with doped amorphous calcium phosphates," *Biomaterials*, 28, 956–965 (2007).

[73] Sheng, Z. Y. and Liu, Y. "Effects of silver nanoparticles on wastewater biofilms," *Water Res*, 45, 6039–6050 (2011).

[74] Liau, S. Y., Read, C., Pugh, W. J., Furr, J. R. and Russell, A. D. "Interaction of silver nitrate with readily identifiable groups: relationship to the antibacterialaction of silver ions," *Lett. Appl. Microbiol.*, 25, 279–283 (1997).

[75] Ewald, A., Hösel, D., Patel, S., Grover, L. M., Barralet, J. E. and Gbureck, U. "Acta Biomaterialia Silver-doped calcium phosphate cements with antimicrobial activity," *Acta Biomater.*, 7, 4064–4070 (2011).

[76] Peetsch, A. *et al.*, "Colloids and Surfaces B : Biointerfaces Silver-doped calcium phosphate nanoparticles : Synthesis , characterization , and toxic effects toward mammalian and prokaryotic cells," *Colloids Surfaces B Biointerfaces*, 102, 724–729 (2013).

[77] Rayman, M. P. "The influence of selenium to human health," *Lancet*, 356, 233–241 (2000).

[78] Whanger, P. D. "Selenium and its relationship to cancer: an update," *Br. J. Nutr.*, 91, 11 (2004).

[79] Wang, Y. *et al.*, "Dual functional selenium-substituted hydroxyapatite," *Interface Focus*, 2, 378–386 (2012).

[80] Cicek, G., Aksoy, E. A., Durucan, C. and Hasirci, N. "Alpha-tricalcium phosphate (α-TCP): Solid state synthesis from different calcium precursors and the hydraulic reactivity," *J. Mater. Sci. Mater. Med.*, 22, 809–817 (2011).

[81] Durucan, C. and Brown, P. W. "A-Tricalcium Phosphate Hydrolysis To Hydroxyapatite At and Near Physiological Temperature," *J. Mater. Sci. Mater. Med.*, 11, 365–371 (2000).

[82] Kannan, S., Mohanraj, K., Prabhu, K., Barathan, S. and Sivakumar, G. "Synthesis of selenium nanorods with assistance of biomolecule," *Bull. Mater. Sci.*, 37, 1631–1635 (2014).

APPENDIX

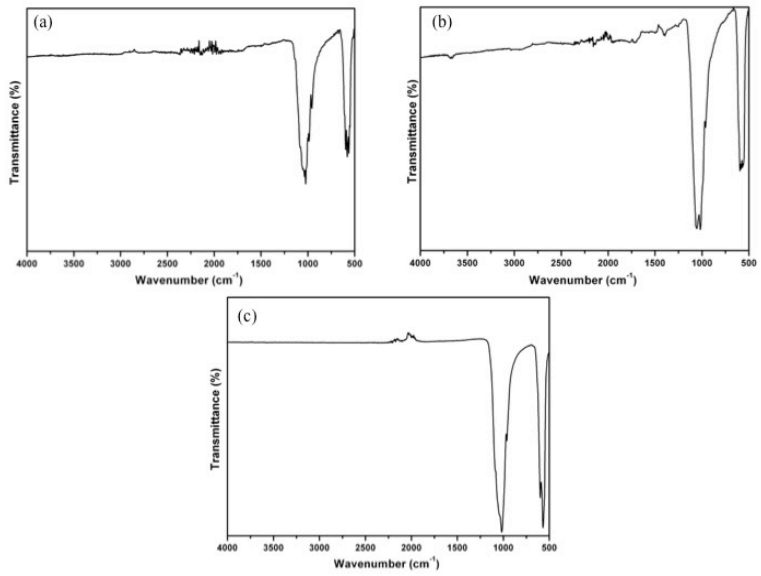

Figure A.1 FTIR spectra of phosphate regions of pure TCP(a), TCP:Se:low(b) and TCP:Se:high(c) in the range of 4000-500 cm^{-1}

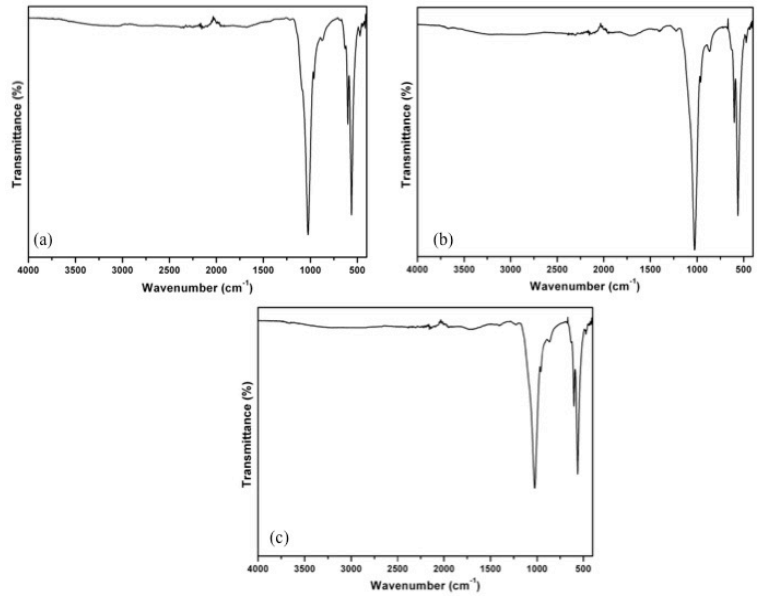

Figure A.2 FTIR spectra of hydration products of pure TCP(a), TCP:Se:low(b) and TCP:Se:high(c) in the range of 4000-450 cm^{-1}